CHAPTER 1.4

Ore Liberation Analysis

Dee Bradshaw, Greg Wilkie, Megan Becker, Cathy Evans, and Norman O. Lotter

Effective ore liberation is at the heart of successful mineral processing; without it, no economic separation process is possible. "Too much" liberation through expensive overgrinding can harm performance; "too little" can cause losses, resulting in the "Goldilocks" effect, where "just right" is required. Therefore, understanding why ore liberation is important; what determines "enough"; and how it can be measured, monitored, and optimized is fundamental to successful mineral processing. The purpose of this chapter is to provide a practical guide of ore liberation analysis, with suitable references to more detailed texts available so that typical problems encountered can be addressed. By understanding the role of liberation and therefore being able to characterize and interpret the "current state" of a circuit, it is possible to diagnose weaknesses and potential for improvement. It is also important to know when liberation is not the reason for poor performance in a circuit.

Bradshaw (2014) identified four steps as being critical to understand and address ore liberation, summed up by the four *I*s:

1. *Information* (appropriate measurements and accurate data)
2. *Interpretation* (correct analysis of information)
3. *Implication* (understanding of the context and application of the information and its interpretation)
4. *Implementation* (execution of the changes necessary to address the implications of the measurement to either the existing circuit or the process design)

If any of these steps are missing, the whole process is threatened, and much of the value can be lost. The first three steps relate to the measurements made on the sample obtained and the knowledge that is being generated, generally at considerable cost and requiring specialist expertise and experience. The fourth step relates to the action that is needed to obtain the value of the investment in the costs of the first three steps. If the fourth step of implementation is not actioned, then the knowledge gained in the first through third steps remains an expensive exercise with little potential value or return on investment (Gu et al. 2014). This chapter does not deal with the sampling methodology needed to obtain a representative sample, although it is acknowledged that no amount of measurement or interpretation can compensate for mistakes at this level (Gy 1979).

This chapter is structured to answer five questions:

1. What is liberation, and why is it critical to mineral processing?
2. How is liberation measured and modeled?
3. What is the best way to report liberation information?
4. When is there enough liberation?
5. How are liberation problems diagnosed, and how are improvements proposed?

The first question deals with the importance of liberation and how it is achieved. The second question deals with the various measurements that can be used and each one's limitations or constraints. The most effective reporting on these measurements depends on the questions being asked and the budget available, as addressed by the third question. The fourth question deals with the drivers that determine "enough." Case studies are cited to illustrate the value of diagnosing and addressing inadequate liberation to answer the fifth question.

WHAT LIBERATION IS AND WHY IT IS CRITICAL TO MINERAL PROCESSING

In mineral process engineering, the material being treated is in the form of either a particulate stream or a lot containing valuable minerals and minerals of no value. To separate these two categories into a valuable concentrate and a less valuable reject product, it is first necessary to liberate one from the other. *Mineral liberation* can be defined as the extent to which the particles are made of discrete mineral grains. If a particle is composed of one mineral only, it is regarded as

Dee Bradshaw, Emeritus Professor, Department of Chemical Engineering, University of Cape Town, Cape Town, South Africa
Greg Wilkie, Program Coordinator, CRC Ore, Brisbane, Queensland, Australia
Megan Becker, Associate Professor, Department of Chemical Engineering, University of Cape Town, Cape Town, South Africa
Cathy Evans, Senior Research Fellow, Julius Kruttschnitt Mineral Research Centre, Brisbane, Queensland, Australia
Norman O. Lotter, President, Flowsheets Metallurgical Consulting Inc., Sudbury, Ontario, Canada

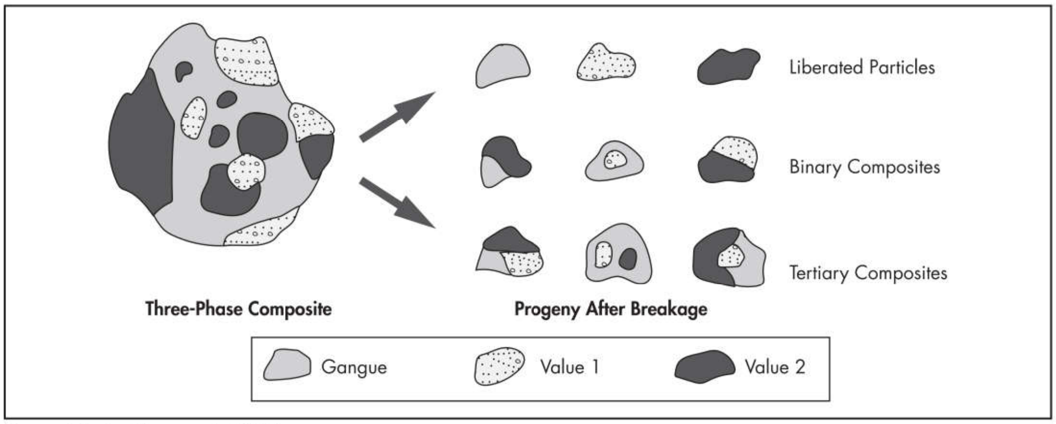

Source: Napier-Munn et al. 2005

Figure 1 Mineral associations in daughter particles from breakage of a complex ore

	Which unliberated particle texture allows the valuable phase to be recovered? (All particles are the same grade.)		
Typical particles of valuable (dark phase) and gangue (light phase) shown in cross section	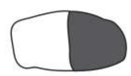	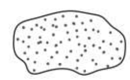	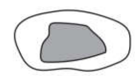
By flotation	✓ Recovered	✗ Not recovered	✗ Not recovered
By density separation	✓ Recovered	✓ Recovered	✓ Recovered
By leaching	✓ Recovered	✗ Not recovered	✗ Not recovered

Source: Evans and Morrison 2016

Figure 2 Schematic showing how ore texture affects liberation and recovery by different processes

fully liberated. Composite particles are made up of mixtures of mineral grains, and a locked particle refers to one having no surface exposure of the selected mineral. Thus, a feed stream to a separation unit contains a distribution of particles of a range of sizes and liberation, and this distribution determines the range of particle properties and the maximum potential for separation success. A stream of well-liberated particles—with the value and gangue minerals in different classes of particles—will separate sharply, whereas a stream of composite particles will not. Figure 1 illustrates the products from rock fragmentation and shows that the daughter fragments of a complex ore can be liberated particles, binary composites, or tertiary composites.

The different processes that the ore is being prepared for require different amounts of liberation to be effective, as shown in Figure 2. Although the amount of valuable mineral in the three examples is similar, the response to the different processes is not because of the difference in texture. Texture, in this context, describes the spatial arrangement, orientation, shape, size, and interrelationships of the constituents in the ore, which include both value and gangue minerals and the mineral aggregates. Textural characterization has been fundamental across the geoscience disciplines, and its application extends throughout the disciplines of mining, mineral processing, and metal extraction, particularly affecting breakage and subsequent liberation (Petruk 2000).

Of particular importance is the surface exposure of the selected or valuable mineral relative to the unwanted gangue mineral. Flotation, for example, is based on the surface properties and requires more of the exposed mineral surface than leaching. There are other factors that can reduce the separation achieved, depending on which separation process is being used (e.g., flotation, gravity leaching). In the case of flotation, these include factors that affect the surface of the particles, such as particle oxidation or surface coatings by fine gangue particles or problems in the equipment operation. Density separation depends on the differences in the particle specific gravity and not the surface properties. Particles can be separated based on their relative movement in response to the force of gravity and one or more other forces (e.g., centrifugal forces, magnetic forces, buoyant forces, or drag forces). This generally takes place in water or in a viscous medium such as heavy media (also known as heavy media separation).

The flotation rate is highly dependent on particle size (Trahar 1981; McIvor and Finch 1991), with ore liberation as an underlying consequence of size. At finer sizes, the particles will tend to be more liberated and will be less liberated at coarser sizes. Figure 3 shows that the recovery is reduced in the finer and coarser sizes. Thus, flotation performance depends on both size and liberation, although they are not the only factors that must be considered.

Figure 4 shows that complete liberation does not guarantee complete recovery. The liberated minerals have to be concentrated in an optimal performance size range by the grinding circuit. Sutherland (1989) identified the interaction between mineral liberation and particle size by demonstrating the different recovery behaviors of chalcopyrite-bearing particles of different sizes with similar liberation characteristics. Figure 4 shows that at the same degree of liberation, coarse particles floated more slowly than intermediate-sized particles but that poorly liberated particles of optimum flotation size could float more rapidly than liberated coarse particles. In some instances, additional collector is added to improve the recovery of coarse liberated particles, but this also leads to the recovery of composite particles, leading to unselective recovery and lower grades.

Apart from different size-by-size recoveries by liberation class, different sulfide minerals present different size-by-size recovery curves (Jowett 1980). An extract of these data is shown in Figure 5.

Methods to directly measure the grain size distribution (GSD) of minerals within a polished section using scanning electron microscopy with energy-dispersive X-ray spectrometry (SEM-EDS) techniques have been developed. Miller and Lin (1988) noted that ores with smaller grain sizes—often measured as the equivalent circle diameter—are indicative of a more disseminated mineral texture.

The specified particle size at which the required degree of liberation occurs depends on

- The original ore texture and GSD of the minerals making up the ore,
- The economical balance between the cost of grinding more finely and the value of increased recovery and concentrate quality (grade, impurities), and
- The separation process selected.

The contribution of texture to liberation was first documented by Gaudin (1939). He noted its effect on liberation and discovered that the size of the target mineral grain influenced the way in which it liberated during grinding. Figure 6 shows his four textures, classified as (1) simple texture, (2) coated or rimming, (3) disseminated or emulsion, and (4) stockwork or veining. Gaudin noted that types 1 and 4 are expected to behave in accordance with the relative abundance of the phases present. Type 2, on the other hand, would not be expected to respond as well as the relative abundance of the minerals present would suggest; instead, it would respond in proportion to the makeup of the exposed particle surface area. Particles representing type 3 typically respond to flotation as one would expect the host phase to respond. In this case, the target mineral is at very low quantities. For intergrowth types 2 to 4, downstream liberation through regrinding is also significantly more challenging compared to the simple texture in type 1. Knowledge of the presence of these intergrowth classes is thus important to understand the processing challenges of ores.

As an alternative to estimating the GSD for a mineral, the phase-specific surface area (PSSA) of that mineral has been shown to have very strong correlations to processing

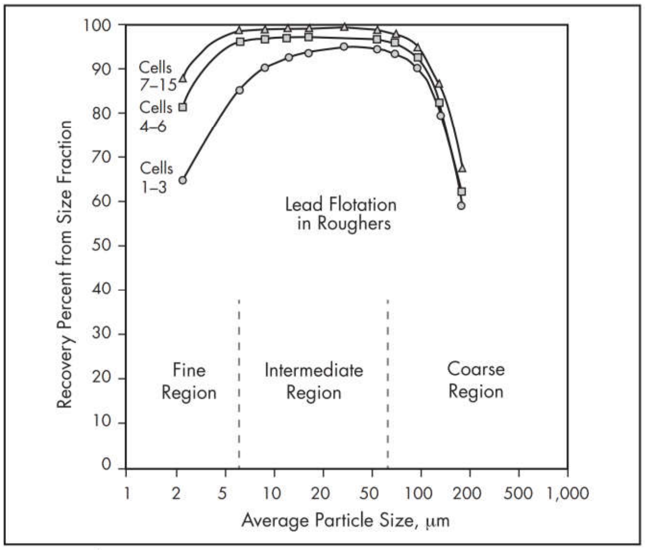

Source: Trahar 1981

Figure 3 Cumulative recovery down the flotation bank at Broken Hill South Ltd. showing the reduced recoveries at fine and coarse sizes

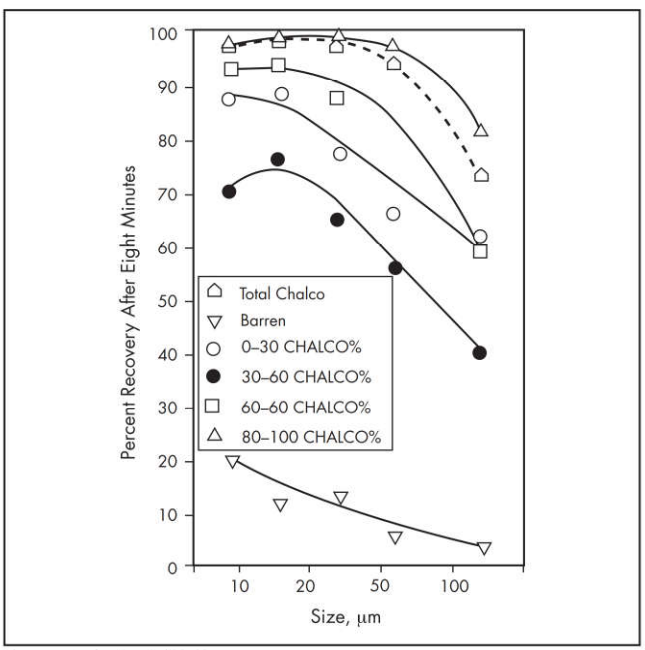

Source: Sutherland 1989

Figure 4 Effects of particle size and liberation on chalcopyrite flotation after 8 minutes

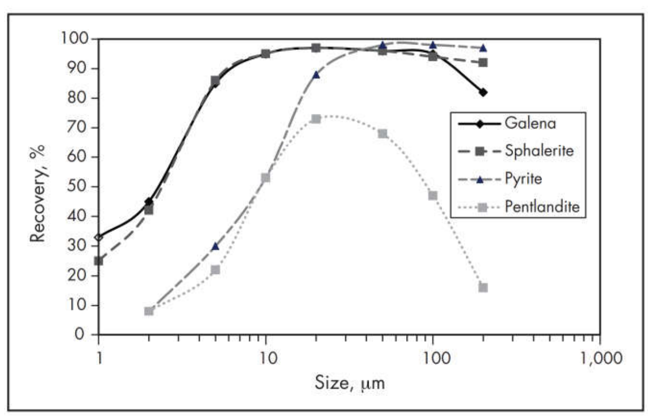

Source: Jowett 1980

Figure 5 Size-by-size recovery curves for different minerals

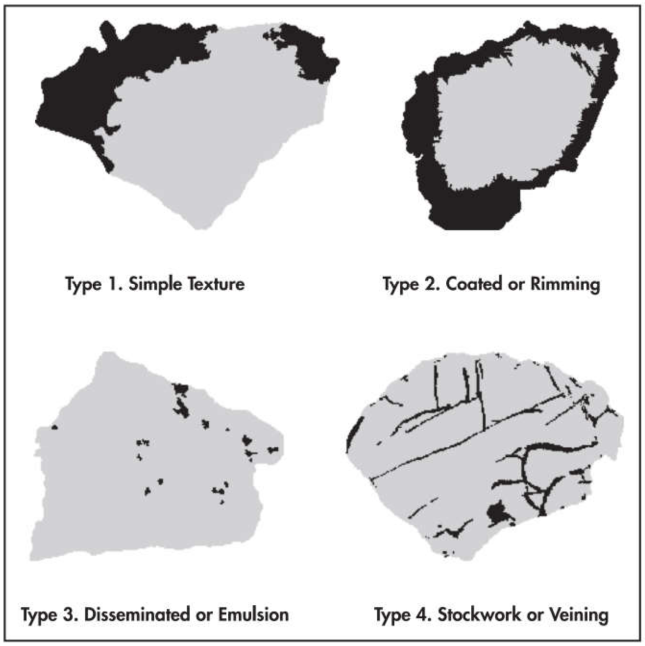

Source: Vos 2017

Figure 6 Examples of SEM-polished section images showing the four intergrowth textures defined by Gaudin (1939) that influence mineral processing

characteristics (Jackson et al. 1988; Sutherland et al. 1991). This quantity, when determined from sectioned images, measures the surface area per unit volume of all mineral grains of a particular phase per total surface area for that phase. A higher PSSA value for a measured population of particle sections indicates finer mineral grain inclusions and hence has a correlation with GSD estimations.

Liberation is achieved through size reduction of the ore. The first size-reduction step is blasting in the mine. In some cases, depending on the ore texture and properties, it is possible to liberate barren gangue material even at large sizes, and this can be treated accordingly. The next step is comminution, which is the most energy-intensive part of the process. It consists of a series of milling and classification units to reduce the feed stream to a specified particle size distribution. This is generally predetermined for a particular ore type to generate the appropriately liberated particles suitable for the specified separation process.

HOW LIBERATION IS MEASURED AND MODELED

Liberation Measurement Techniques

Because mineral liberation depends on the relationship between mineral grain size and particle size, liberation is characterized by the mineral grade per size fraction. The first step is to obtain different size fractions either by physical screening or by using heavy liquid separation or elutriation to obtain particles falling into narrow density classes (Gaudin 1939; Sutherland et al. 1988). There is, however, a known limitation with the latter approach when the density and size of particles vary. Particles of different sizes and density can have the same overall mass and be collected in the same fraction obtained when using a cyclosizer. At finer size fractions where the particle size is equal to or less than the mineral grain size, the particle will be fully liberated. Conversely, at coarser size fractions where the particles contain various mineral grains, the particle will be less liberated. Thus, the first proxy for liberation is the varying chemical assay or grade with particle size. In many cases, characterizing the variation of grade with particle size is enough to characterize where the extent of liberation can become a problem, and more sophisticated, expensive measurement is not necessary.

Formal mineral liberation measurements require observing and characterizing the mineral grain distribution in the particles that make up the stream to be separated. These fall into two main categories:

1. Two-dimensional (2-D) measurements obtained from polished sections of ore particles
2. Three-dimensional (3-D) measurements obtained from whole ore particles by either physical measurement or nonintrusive methods such as 3-D tomography

Within these two categories, the measurement techniques are further subdivided into classifications based on the technology platform being used. Two-dimensional instruments are also known as image analysis instruments and include optical microscopy and SEM-EDS systems. Both techniques can be automated; the former uses light microscopy to identify minerals, whereas the latter uses characteristic X-rays measured from an electron beam to identify minerals.

Three-dimensional techniques include the recently developed computer-aided tomography that has been applied to liberation studies to obtain 3-D images of whole ore particles to overcome the effects of stereological bias, which is described in the next section. The preferred technology platform is the X-ray micro-computed tomography, or μCT (Miller et al. 1990; Morrison and Gu 2016).

Each of the aforementioned techniques has their own individual strengths and limitations; these techniques are discussed in greater detail in the study by Wilkie (2016). Image analysis methods using optical and SEM-EDS platforms are by far the most widely used and most mature of the technologies. Automated image analysis instruments (e.g., Quantitative Evaluation of Minerals by Scanning Electron Microscopy [QEMSCAN], Mineral Liberation Analyzer [MLA], Mineralogic, and TESCAN Integrated Mineral Analyzer [TIMA-X]) are now widely available as commercial products and can be used directly on the site of a mineral processing operation. Their fundamental limitation is that measurements of liberation in polished sections are fundamentally biased (see the following section). There is a substantial body of work in the literature—most notably from King (1983), Barbery (1987), Gay (1996), Leigh et al. (1996), and Latti (2006)—that attempts to transform 2-D measurements into three dimensions. Despite this work, most liberation measurements performed by commercial image analyzers present untransformed 2-D liberation data, and the effect of the bias is often unknown in three dimensions. In practical terms, use of the 2-D data for liberation is useful, and the following typical categories of liberation are successfully used to interpret the flow-sheet and processing implications of the data (Lotter et al. 2002, 2018a):

1. Liberated particles are fragments in which more than 90% of the particle is made up of the mineral of interest.
2. Middling particles are those fragments in which between 30% and 90% of the particle is made up of the mineral of interest.

3. Locked particles are those fragments in which less than 30% of the particle is made up of the mineral of interest.

With regard to 3-D techniques, the physical separation of particles into grade classes using heavy liquid separation is the oldest and simplest technique. This technique works well on simple binary ores where there are two minerals with large differences in density. The technique is less useful on ores where there are a large number of minerals with varying densities present in the particle. X-ray µCT has the ability to directly measure the 3-D liberation of particles, thus overcoming the stereological bias of 2-D image analysis instruments (Miller et al. 2009). The current generation of X-ray µCT instruments is limited, however, in terms of both spatial resolution and phase resolution, so small objects in a particle of complex mineralogy are difficult to resolve. Heavy liquid separation is also more problematic for separations of finer particles.

Stereological Bias in 2-D Measurements of Liberation

There are several methods available for the measurement of liberation; however, the industry standard is based on 2-D image analysis instruments. Therefore, it is important to discuss the effects of stereological bias when using 2-D image analysis liberation data. Figure 7 shows a schematic that demonstrates the stereological bias associated with sectioned measurements.

In this stylized view, a locked particle containing three phases (A, B, and C) is mounted in a 3-D cylinder and sectioned at two points through the cylinder. The two sections on the right of the cylinder show two different particle compositions; the first (through B) shows a completely liberated section of Phase B, whereas the second (through C) shows a particle of Phase C completely rimmed by Phase B. Both of these sections were obtained from the same locked particle, which demonstrates the fundamental stereological bias. A locked particle can be sectioned into a variety of liberated and locked sectional views, whereas a liberated particle can only be sectioned into liberated sectional views. Hence, there is a fundamental bias in overestimating liberation from 2-D measurements.

Work by several authors (Stewart and Jones 1977; Miller and Lin 1988; Spencer and Sutherland 2000; Latti 2006) has shown that the degree of stereological error is variable and depends on the texture of the ore as well as the degree of liberation present. Figure 8 shows a representation of the stereological bias associated with varying degrees of textural complexity as described by Spencer and Sutherland (2000).

Wilkie (2016) analyzed this diagram in the context of using image analysis methods for predicting the liberation of

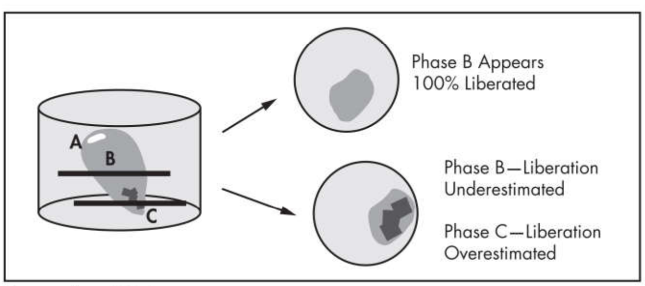

Source: Latti 2006

Figure 7 Stereological bias obtained from sections through a locked particle

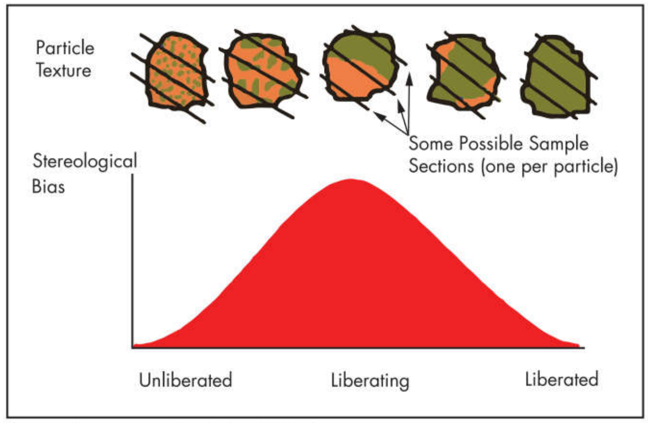

Source: Spencer and Sutherland 2000

Figure 8 Stereological bias associated with textural complexity

gangue for ore-sorting applications. His analysis of the schematic is summarized as follows:

> In essence, the greater the complexity inherent in the texture, the less bias is seen in the untransformed one- and 2-D data. Hence for complex disseminated textures measured at coarse particles, little or no stereological bias is present in the data whilst the presence of simple textures and barren matrix is indicative of stereological error.

The reference to one-dimensional data in this quotation is the use of linear measurements of particle grades performed on image analysis instruments. We can therefore expect to see little or no stereological bias in sample streams that are largely unliberated or highly liberated. The main streams we need to carefully assess are those that contain a large proportion of simple binary particles.

In addition to textural complexity, the stereological bias may also be exacerbated by the modeling procedures used to quantify liberation from image analysis measurements. Latti (2006) concluded that "in multiphase systems evaluated, the stereological bias is small when comparing the overall two- and three-dimensional liberation distributions but significant when liberation distributions are determined from one dimensional data" and that "it was also found that the practice of combining minerals into groups in order to simplify the problem may increase the stereological bias, particularly for particle sizes that are greater than the liberated size of the majority of the minerals in a given dataset." In essence, the practice of modeling multiphase binary particles as simplified binaries between the phase of interest and gangue may result in reallocating particles to the left of the curve in Figure 8 to the middle of the curve, resulting in a high degree of stereological bias. This is due to the modeling method used rather than inherent bias in the raw image analysis method.

In summary, although the debate between researchers on the extent of the liberation bias in 2-D measurements of liberation remains largely unresolved, the work by Latti (2006) and Spencer and Sutherland (2000) indicates that the bias is problematical in a limited set of particle textures, predominantly simple textures in binary particles. To this end, it is common practice in the mineral processing industry to use untransformed 2-D liberation data for modeling liberation around a circuit because the use of stereological transforms is complex and can often exacerbate the bias, as discussed previously. Provided that the untransformed data are viewed in relative terms as opposed to absolute terms (i.e., used to measure changes in liberation as opposed to absolute values of liberation), the use of untransformed liberation data still provides useful insights into the comminution behavior of mineral streams in a unit operation.

Sample Methodologies for Liberation Analysis

The general framework for preparing samples for liberation analysis is common across the various mineral processing operations, including flotation, gravity separation, and leaching. All applications are measured on a size-by-size framework for three main reasons. The first is that most mineral separation techniques perform differently on different particle sizes, as shown by Figures 1 and 2 for flotation. Second, the stereological bias, as shown in Figure 8, is significantly reduced when narrow size fractions are measured. It is typical to use a root-two or factor-two series of screens when classifying the sample into narrow size fractions. The third reason is that the presentation of the sample to a SEM in known size classes allows the application of quality control to disqualify certain particles in view of the SEM because they are either coarser or finer than the stated size limits of that size class. The general framework may be summarized as follows:

1. Representative sampling of the product stream
2. Subsampling of the product stream using rotary rifflers and classification of the stream aliquot into specific size fractions
3. Subsampling of product size fraction and mounting into polished sections
4. Measurement of polished sections by selected image analysis technique (optical, SEM-EDS)
5. Allocation of particles into grade classes (typically 12 grade classes of 10% intervals) ranging from the barren class (0% value) to the fully liberated class (100% value)
6. Analysis, data validation, interpretation, and reporting of changes in liberation across the unit operation

There are, however, several differences in the specific application, primarily due to grade and particle size. To build a statistically relevant grade distribution across 12 grade classes, typically more than 100 particle sections need to be allocated across the 12 grade classes. Lower grades and coarser particles therefore require more polished sections to achieve the particle statistics required for quantitative liberation measurements (Wightman et al. 2016). Table 1 shows a typical experimental design for a liberation analysis around a porphyry copper flotation circuit.

Typical porphyry copper concentrators have a flotation P_{80} feed size of around 150–200 µm, and a factor-two series of size fractions results in six size fractions being analyzed. Because of the grade differences among the feed, concentrate, and tailings stream and the number of value-bearing particles in the various size fractions, concentrate streams require only one polished section to be measured across all size fractions, whereas feed and tailings streams require more polished sections in the coarser size fractions to be measured. This experimental design will ensure that assay reconciliation can be achieved across all size fractions and provide a statistically relevant population of value-bearing particles being measured to build the particle grade distribution.

Table 1 Number of polished sections in each size fraction

		Size Fraction, µm					
Product Stream	**Grade, %**	**−10**	**−20**	**−38**	**−75**	**−150**	**+150**
Feed	0.5–1	1	1	1	2	2	3
Concentrate	20–40	1	1	1	1	1	1
Tail	0.05–0.1	1	1	2	3	4	6

To understand and characterize the statistical robustness of the liberation measurements, Leigh et al. (1993) proposed estimating the confidence limits of liberation measurements made on ore particles using the "bootstrap" technique. This technique was extended to measurement of mineral grain size by Evans and Napier-Munn (2013). A simple analytical technique also proposed by Leigh et al. (1993) has been applied in a case study described by Lotter et al. (2018b) to estimate the confidence limits of liberation measurements on concentrate and tailings samples of a chalcopyrite ore. In the case study example, approximately 15,000 particle sections were measured for the concentrate sample (grade 15.5% Cu) and 20,000 particle sections were measured for the tailings sample (grade 0.11% Cu). The estimated confidence intervals for the two samples are shown in Figure 9, which clearly shows that although more particle sections were measured in total for the low-grade sample, the confidence limits are much larger for this sample because the low grade of the tailings stream results in fewer particles of interest being present in each particle composition class. To overcome this problem, specialized measurement routines for low-grade samples have been implemented in most automated SEM-EDS-based mineralogy systems to specifically search for and measure only particles that contain the minerals of interest. Using these specialized routines maximizes the number of particles containing the minerals of interest measured in standard measurement times and increases the confidence in the resulting liberation data.

Errors in Liberation Measurements

Whereas correct sampling of particulates provides true sample material with known confidence limits to the mineralogist, the subsequent mineralogical measurements are also subject to measurement errors (Lotter et al. 2018b). Early methods to estimate the errors in the measurement of mineral proportions using optical microscopy were published by Chayes (1944, 1945) and Van der Plas and Tobi (1965). While the development of automated mineralogy systems in recent years has made it easier to collect larger volumes of data, these measurements are still affected because the measured properties of a subsample of particles (typically around 10,000 to 30,000 particles) are used to represent the larger population from which they were sampled. In the early days of these automated mineralogy systems, Leigh et al. (1993), working with QEMSCAN data, developed an analytical method to estimate the confidence intervals for liberation data in cumulative liberation distribution (also known as the cumulative liberation yield) form. They noted that the bootstrap method of Efron (1987) would give a definitive answer, but at that time, the computationally intensive bootstrap technique was not practical to apply. Now, the restrictions imposed by lack of computing power no longer apply and the bootstrap technique has

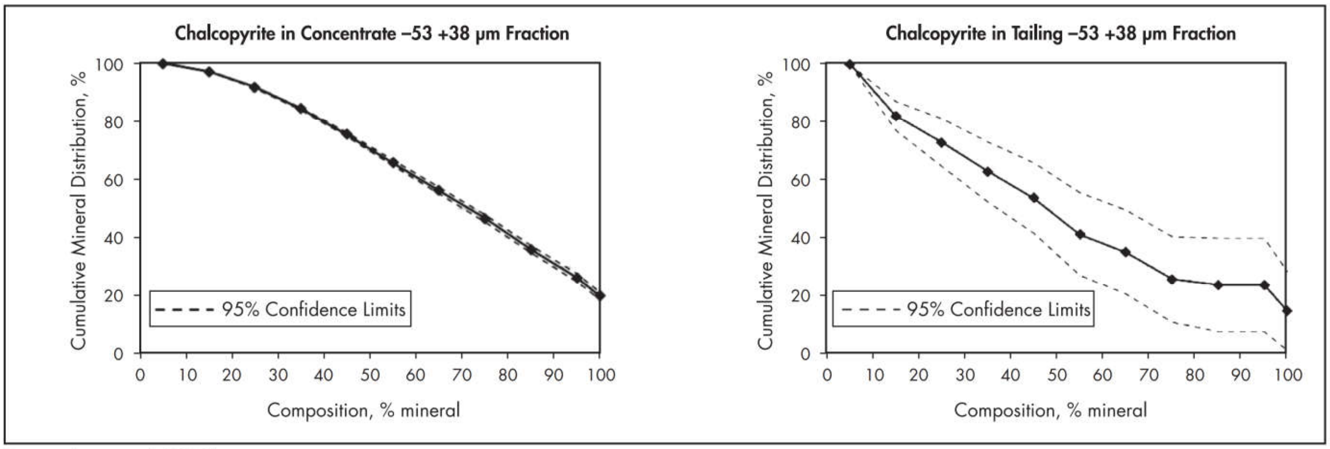

Source: Lotter et al. 2018b

Figure 9 Comparison of the confidence intervals on mineral liberation in concentrate and tailings samples

been successfully used to estimate confidence intervals for mineral GSDs (Evans and Napier-Munn 2013) and for non-cumulative liberation distributions (Mariano and Evans 2015) from MLA data. Typically, in this application, larger data sets are associated with higher levels of confidence in the liberation measurement.

The analytical approach developed by Leigh et al. (1993) uses the following equation to estimate the 95% confidence interval, *CI*, at particle composition *C* as a function of the number of particles in the liberation classes:

$$CI_C \approx 1.96 * \left(1.25Y_C^2(1-Y_C)^2\left(\frac{1}{N_0}+\frac{1}{N_1}\right)\right)^{0.5} \quad \textbf{(EQ 1)}$$

where

Y_C = value of cumulative liberation distribution at particle composition *C* (as a proportion)

N_0 = number of particles in composition classes with composition less than *C*

N_1 = number of particles in composition classes with composition greater than or equal to *C*

A case study on process streams from a copper concentrator from Lotter et al. (2018b) illustrates the importance of understanding the confidence intervals that apply to liberation data. In this example, the liberation distribution of chalcopyrite has been measured in a concentrate and a tailings stream, and after applying Leigh et al.'s (1993) analytical method to the liberation data for these high-grade and low-grade samples presented in Tables 2 and 3, it is clear that the estimated confidence intervals are much wider for the low-grade material that has fewer observations of chalcopyrite.

When the estimated confidence limits are included in the plots of the cumulative liberation distributions of chalcopyrite in the two streams, as in Figure 9, the difference between the low-grade and high-grade streams is obvious. The level of confidence in the liberation data for the lower-grade sample of tailings with a copper grade of 0.11% is considerably less than the confidence in the higher chalcopyrite content concentrate sample that has a copper grade of 15.5%. The low chalcopyrite content of the tailings stream results in fewer chalcopyrite-bearing particles in each particle composition class (N_1 in the equation of Leigh et al. [1993]) and this is the reason for the wide confidence intervals. The difference in confidence levels, which results from lower numbers of particles in each liberation class in low-grade streams, is the reason why modern automated mineralogy systems include specific measurement procedures to scan for and only measure particles that contain the minerals of interest. This approach maximizes the number of particles containing the minerals of interest that are measured when analyzing low-grade samples and increases the confidence that the end user can have in the resulting liberation distribution data.

The experimental design shown in Table 1 also works well for sulfide nickel operations in which the grade and particle sizes can be similar to those of porphyry copper operations. Lead/zinc flotation operations typically have much higher feed and tailings grades (up to an order of magnitude higher), so the number of polished sections in the coarser fractions can be reduced substantially while still maintaining assay reconciliation and statistically reliable populations of value particles for particle grade distributions.

In the case of leaching operations, the problems associated with particle size are further exacerbated by the coarser feed P_{80} that is typical for leaching. Leach feed particle sizes range from approximately 2 mm to run-of-mine consisting of uncrushed material. Latti and Wilkie (2016) outline an experimental design for a leaching circuit composed of 100% passing 12-mm material. In this study, the size fraction grid consisted of five size fractions represented by the +14 mm, +8 mm, +1 mm, +150 µm, and –150 µm fractions. Sample preparation followed the aforementioned generic workflow with up to 12 polished sections being prepared in each size fraction. Standard 30-mm mounts were prepared for the fractions finer than 4 mm, whereas specially prepared 100-mm square mounts were prepared for the fractions coarser than 4 mm to obtain a reasonable population of particles in the polished section. Figure 10 shows examples of the large-area polished sections from the study by Latti and Wilkie (2016). As with concentrator applications, the polished sections are measured by automated image analysis instruments to obtain the particle grade distribution and model the liberation of the ore at discrete particle sizes.

Modeling of Liberation

The earliest work on liberation modeling was conducted by Gaudin (1939), who conceptualized the liberation process

Table 2 Confidence interval estimation for a concentrate sample (–53 +38 µm, 15.5% Cu)

Mean Grade of Composition Class	Cumulative Distribution of Mineral	Number of Particles in Class	N_0	N_1	95% Confidence Interval	Lower Confidence Interval	Upper Confidence Interval
Barren	100.0	6,185	—	—	—	—	—
5	100.0	2,624	6,185	10,518	0	100.0	100.0
15	97.2	1,484	8,809	7,894	0.09	97.1	97.3
25	91.8	1,222	10,293	6,410	0.26	91.6	92.1
35	84.4	1,006	11,515	5,188	0.48	83.9	84.9
45	75.5	906	12,521	4,182	0.72	74.8	76.3
55	65.8	685	13,427	3,276	0.96	64.8	66.7
65	56.3	580	14,112	2,591	1.15	55.1	57.4
75	46.6	489	14,692	2,011	1.30	45.3	47.9
85	36.0	400	15,181	1,522	1.36	34.7	37.4
95	26.2	235	15,581	1,122	1.31	24.8	27.5
100	19.9	887	15,816	887	1.20	18.7	21.1

Source: Lotter et al. 2018b

Table 3 Confidence interval estimation for a tailings sample (–53 +38 µm, 15.5% Cu)

Mean Grade of Composition Class	Cumulative Distribution of Mineral	Number of Particles in Class	N_0	N_1	95% Confidence Interval	Lower Confidence Interval	Upper Confidence Interval
Barren	100.0	19,908	—	—	—	—	—
5	100.0	62	19,908	102	0	100.0	100.0
15	82.1	12	19,970	40	5.10	77.0	87.2
25	72.9	4	19,982	28	8.19	64.7	81.1
35	62.7	4	19,986	24	10.46	52.3	73.2
45	53.7	6	19,990	20	12.19	41.5	65.9
55	41.2	2	19,996	14	14.19	27.0	55.4
65	35.1	4	19,998	12	14.41	20.7	49.5
75	25.7	2	20,002	8	14.80	10.9	40.5
85	23.7	0	20,004	6	16.16	7.5	39.8
95	23.7	2	20,004	6	16.16	7.5	39.8
100	14.7	4	20,006	4	5.10	1.0	28.4

Source: Lotter et al. 2018b

associated with size reduction of the rock as a cubic aggregate containing both valuable and waste mineral grains. The aggregate is then broken into particles of uniform size by a cubic fracture lattice that is randomly superimposed on the aggregate parallel to the grain lattice. This model was further developed by Wiegel and Li (1967) to produce the Gaudin random liberation model, which is conceptualized in Figure 11.

Both Gaudin (1939) and Wiegel and Li (1967) derived a set of equations to calculate the proportion of liberated values, liberated waste, and locked waste and value minerals, producing the plot shown in Figure 12.

In the case represented by Figure 12, the diagram represents the proportion of liberated values, liberated waste, and locked values and waste for an ore containing 25% values. The diagram is divided into three distinct fields:

1. Coarse particles (grain size–particle size ratio < 1) where locked values and waste dominate the population

Source: Latti and Wilkie 2016

Figure 10 Large-area polished sections for coarse particles

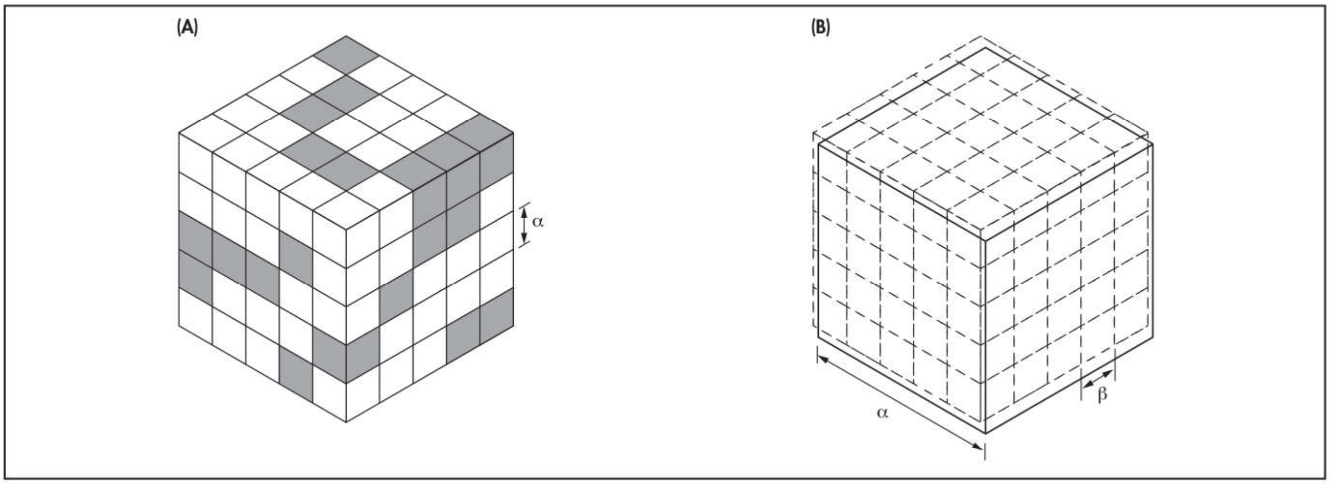

Source: Wiegel and Li 1967

Figure 11 (A) Random arrangement of mineral grains and (B) fracture of a single mineral grain into particles

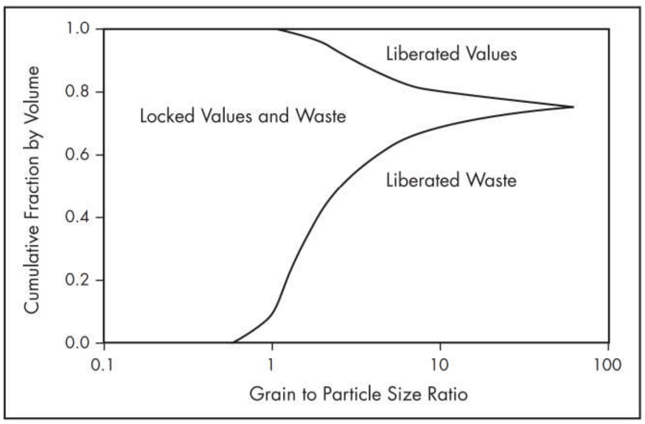

Source: Wiegel and Li 1967

Figure 12 Fraction of locked and liberated particles versus grain size–particle size ratio for an ore with 0.25 fraction values

2. Intermediate particles (grain size–particle size ratio ≈ 1) where there is a mixture of liberated values, liberated waste, and locked values and waste
3. Fine particles (grain size–particle size ratio > 1) where liberated waste and liberated values dominate the population

Other researchers in the field of liberation modeling who have taken various mathematical, theoretical, or combined approaches include King (1982, 1990), Barbery (1984, 1991), Gay (1996, 2004), Evans (2002), Evans and Morrison (2016), Subasinghe and Dunne (2016), and Wilkie (2016). All the methods are aimed at predicting the particle grade distribution within a given particle size class but differ in the mathematical approach that they use to quantify the distribution. Many of these methods rely on image analysis measurements that require stereological correction.

King's (2000) approach, for example, is to model the particle grade distribution with a beta distribution, which is widely used in mathematical statistics. The particle grade distribution is conceived as being made up of three types of particles:

1. Liberated gangue particles, denoted as L0
2. Liberated value particles, denoted as L1
3. Mixtures of gangue and value particles that have a grade distribution given by the probability distribution density function $p(g)$, which is modeled by the beta distribution

By contrast, Barbery's (1984, 1991) method is based on the concepts of geometric probability originally developed by Davy (1984). Barbery's method relies on three fundamental assumptions:

1. Breakage is assumed to be random, uniform, and isotropic.
2. A Poisson mosaic or Boolean texture is assumed.
3. A particle shape model is also assumed.

The value of this liberation modeling is that the proportion of each particle class can be calculated for any given particle size and grain size inherent in the ore. An important aspect to the incorporation of the liberation of particles into process modeling and simulation is the mass balancing of the data. Methods have been developed to mass balance particle liberation data in process streams (Lamberg and Vianna 2007), and a simulation framework has been developed to provide simulations of comminution, liberation, and separation in one integrated system (Evans et al. 2013).

THE BEST WAY TO REPORT LIBERATION

Optical

Traditional optical microscopy methods generally allocate ore-bearing particles into categories represented by liberated particles, binary particles with other minerals, and ternaries that are locked with two or more minerals. This is shown in Table 4, which summarizes the liberation characteristics of chalcopyrite on a size-by-size and overall basis (Henley 1983).

Hence, on an overall basis, 82% of the chalcopyrite is liberated with 6% present as binaries with magnetite, 5% as binaries with pyrite, and 4% present as ternaries. Analysis of the size-by-size distributions shows that between 93% and 100% of the chalcopyrite is liberated in the finer –45-µm size

Table 4 Examples of liberation at the different size fractions

Size Fraction, μm	% Liberated Chalcopyrite	% Chalcopyrite Locked in Binary Particles with ...				% Chalcopyrite Locked in Ternary Particles
		Magnetite	Pyrite	Nonopaques	Pyrrhotite	
+180	45	4	8	22	5	16
–180/+90	50	20	10	10	0	10
–90/+45	88	2	2	0	2	5
–45/+22	93	2	5	0	0	0
–22/+8	95	0	5	0	0	0
–8	100	0	0	0	0	0
Total	(82)	(6)	(5)	(2)	(1)	(4)

Source: Henley 1983

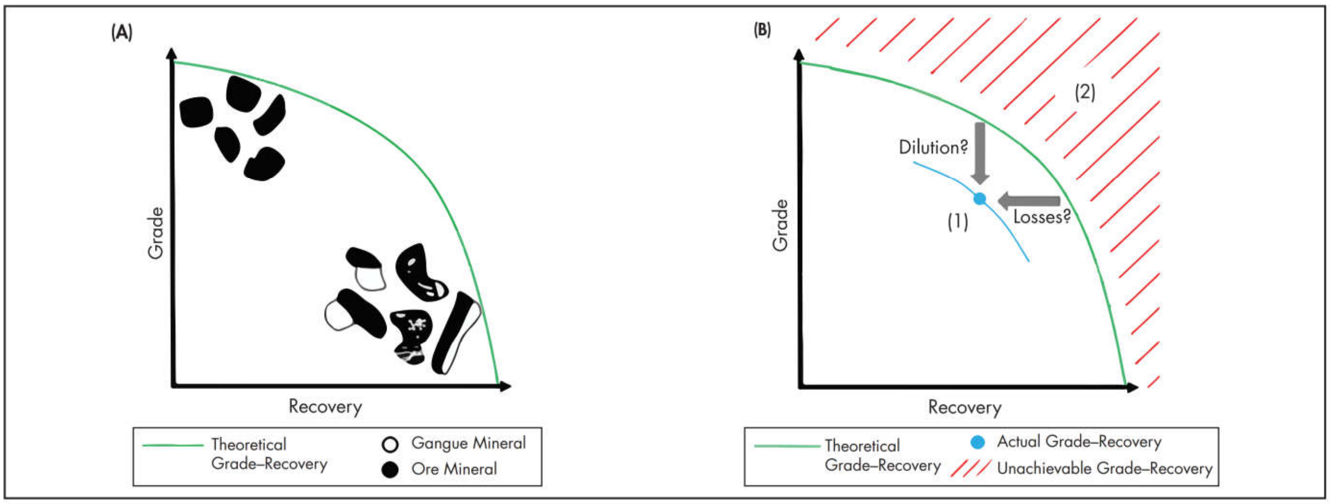

Source: Cropp et al. 2013, reprinted with permission from the Australasian Institute of Mining and Metallurgy

Figure 13 (A) Schematic of the theoretical grade–recovery curve with typical particle images included; and (B) the position of the actual grade recovery relative to the theoretical potential, where (1) operational changes can be made to improve performance and (2) milling and classification changes are needed for improved performance

fractions, with liberation decreasing dramatically to 50% and 45% in the 90- and 180-μm fractions, respectively. These two size fractions show significant proportions of chalcopyrite binaries locked with magnetite, pyrite, and nonopaques along with ternary particles. The overall conclusion is that the chalcopyrite is well liberated in the floatable size ranges but less liberated in the coarser fractions.

Automated SEM-EDS

In addition to the traditional approach of reporting liberation as a proportion of liberated binaries and ternaries, commercial automated SEM-EDS mineralogy instruments have numerous built-in software features to report liberation in several different ways. Furthermore, researchers are developing new and interesting ways to report liberation in a mineral processing context. The following sections illustrate some of these as well as a few newer liberation concepts.

Theoretical Grade–Recovery/Mineral Potential Curve

The mineralogical limit to flotation or theoretical grade recovery is a means of describing or characterizing the recovery of particles based on the ore mineralogy and texture of the ore present in the feed stream. It assumes perfect separation and does not take process kinetics or material recovered by entrainment into account. Therefore, it cannot necessarily be considered a realistic target but does provide the maximum limit. It takes into account the composition of the particles containing the valuable mineral and gives the maximum potential separation of it. The location of the limit is determined by the quality and quantity of composites, as shown in Figure 13.

Figure 13 shows how particle composition defines the theoretical grade–recovery curve. Images of particles are used to show how high recovery of the target mineral will typically also mean recovery of gangue minerals, thus reducing the grade of the concentrate. If there are more composite particles and the feed stream is consequently lower grade, the curve in Figure 13A shifts left (such as in a scavenger stream). Conversely, if it is a stream containing a lot of liberated particles (such as a cleaner stream), the curve shifts to the top right-hand corner.

Figure 13B shows the position of the actual grade–recovery curve relative to the theoretical potential. At point 1, the operational conditions such as reagent addition or circuit modifications can be altered to improve performance, but only to the limit imposed by the curve. If grade recovery above the theoretical curve is required, such as for point 2, then the liberation potential of the feed will need be changed by altering the milling and classification conditions. This curve does not include entrainment or naturally floating gangue, so it will always be an overestimate of what can be achieved practically. The procedure to calculate the theoretical grade–recovery curve is discussed by Johnson (2010).

Cumulative Liberation Yield

The cumulative liberation yield (CLY), as shown in Figure 14, represents the proportion of all of the mineral for a sample contained in particles with a composition greater than some predefined value. For example, CLY90 is the proportion of all of the mineral for a particle contained in particles with a composition greater than 90%. Thus, the CLY cumulates from right to left. An alternate representation of the CLY is to cumulate particles from the lowest quality (least liberated) to highest quality (most liberated), that is, from left to right.

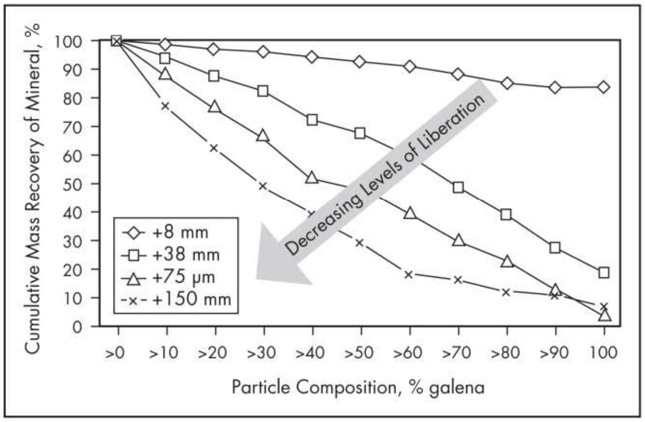

Source: Evans and Morrison 2016

Figure 14 Graphical presentation of particle composition data as a cumulative liberation yield

Liberation and Association

In addition to representing liberation data in discrete categories of particle composition, such as the CLY (Figure 14) or categories of locked–middlings–liberated particles, a user of an automated SEM-EDS instrument is able to interrogate the liberation data to further understand the characteristics of unliberated particles. This could be through visual inspection of the false color particle images provided by the automated SEM-EDS instrument or more quantitative characterization using discrete user-defined categories of interest (Figure 15).

Liberation Spectrum

Wightman and Evans (2013) developed a technique using information obtained from automated SEM-based systems called the "liberation spectrum." This spectrum represents the compositional distribution of a particle population in a form that is useful to mineral processors, particularly to determine grinding targets for separation processes.

Figure 16 shows the graphical relationship of the liberation spectrum by plotting the grade of pyrite containing particles at various particle sizes. It provides insights into the particle size at which liberation begins (point B), above which the linear relationship shows the particle size at which the grains of the mineral of interest remain unbroken (feed grade A). Point C shows the distribution of grain sizes present and whether multiple populations of grain sizes are present in the sample. This type of information can be used to select targets for grind size and includes mineral grade information, which can be used to infer the response to the grind targets.

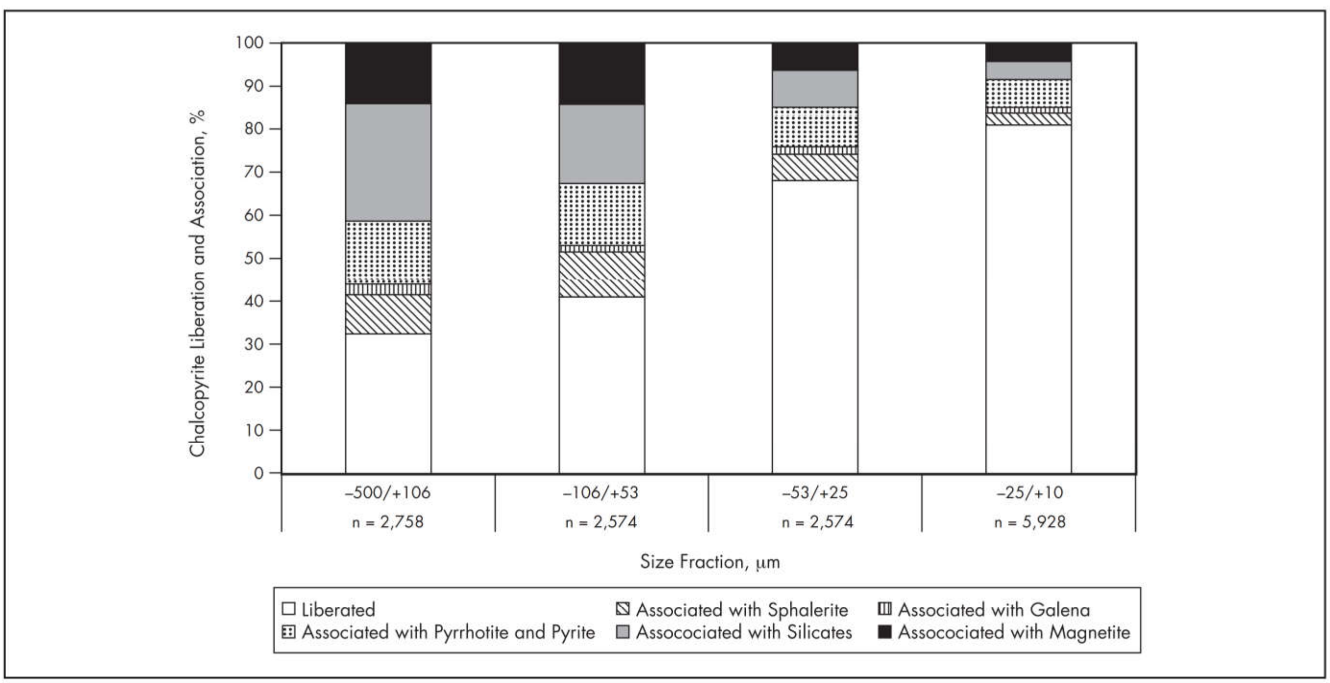

Figure 15 Representation of particle liberation and association on a size-by-size basis (*n* = number of particles measured containing the mineral of interest). The association quantifies the grain boundary characteristics of unliberated valuable minerals with the mineral of interest.

X-Ray Microtomography

The development of the application of X-ray tomography (3-D) to ores and minerals has provided an opportunity to measure mineral liberation (and other characteristics) in three dimensions. These measurements, which were originally developed for medical purposes, have been successful in measuring differences in the density of different minerals nonintrusively (Miller et al. 1990; Evans et al. 2012; Ghorbani et al. 2013; Morrison and Gu 2016). This method has the advantage of removing the effect of stereological bias from measurements of particle liberation. The method also has the advantage of much easier, quicker, and more cost-effective sample preparation in that no polished sections are necessary. The sample size does determine the voxel size obtainable in the output image, and if high resolution is needed, the sample size should be small enough (Morrison and Gu 2016).

The limitations of the measurements also include the lack of elemental determination, and the mineral composition of an ore has to be calibrated using SEM techniques. If the density and resulting X-ray attenuation of minerals are too close, discrimination is difficult, but techniques to address this are being developed. Analytical methods combining the merits of both techniques are also being developed. Large amounts of data are generated, and this requires significant computing power for the reconstruction.

It is anticipated that as software and hardware innovations are developed and computing power continues to increase that this methodology will be developed to give real-time, online liberation measurements of particle streams.

Figure 17 shows that the 2-D measurements overestimate liberation relative to the 3-D measurements, which correlate to the flotation results.

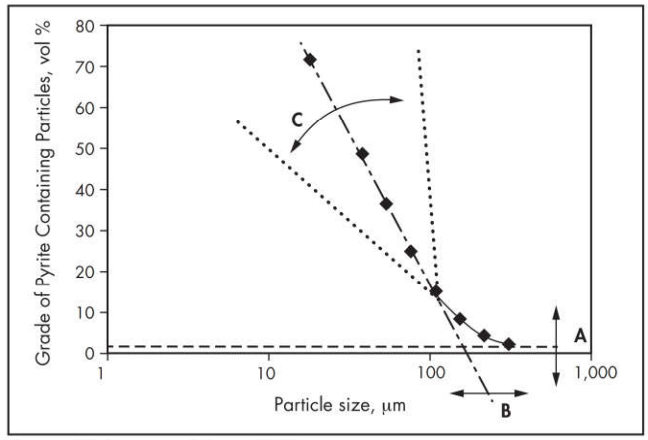

Source: Wightman and Evans 2013

Figure 16 Representation of the liberation spectrum from the automated SEM-EDS measurement, where point A represents the feed grade of the sample, point B represents the size at which liberation begins, and point C indicates the distribution of sizes of the mineral grains

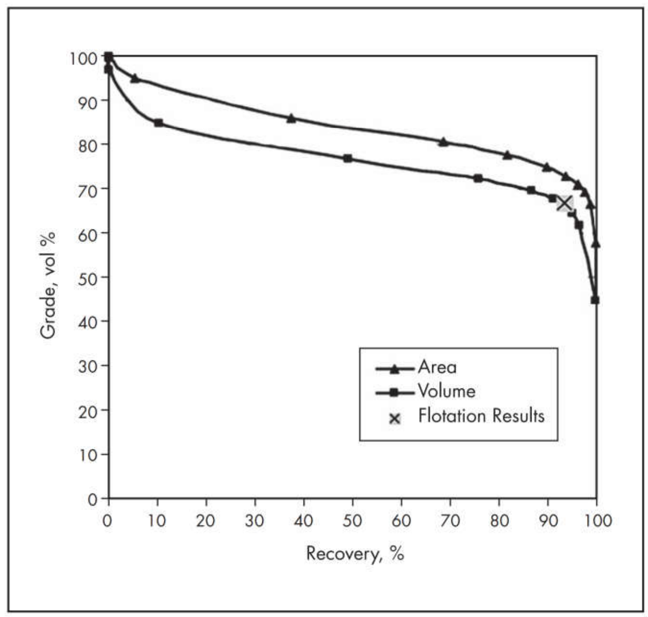

Source: Miller et al. 2009

Figure 17 Difference in theoretical grade–recovery/mineral potential curves for a phosphate ore obtained in two dimensions (area) and three dimensions (volume) as well as the actual flotation results achieved

DETERMINING WHEN THERE IS ENOUGH LIBERATION

Ultimately, the decision on whether there is enough liberation is determined by the mineralogy of the ore and the concentration process being used. Most concentration processes exhibit a size recovery curve, which means that not all particle sizes and particle grades are recovered equally, resulting in a Goldilocks particle size for optimum liberation and recovery. However, there are further technoeconomic (and environmental) considerations that will influence the decisions made regarding the degree of liberation at which a plant will operate, and these need to be taken into account. The following sections describe the need for optimum liberation and particle size for three of the most common extraction processes: flotation, gravity separation, and leaching.

Flotation

The typical influence of mineralogy and texture on flotation performance is summarized in Figure 18; this is accompanied by a schematic showing the size fraction affected.

The losses of valuable mineral and dilution to concentrate in the three major size categories can be commonly attributed to the following:

- Coarse particles can be composites (i.e., contain multiple grains) of value-bearing minerals and gangue minerals. Recovering these particles will increase overall recovery but lower the grade of the concentrate, as the locked, attached gangue will, by necessity, also be recovered. Rejecting these will mean that the grade is not compromised, but the target grains will be lost to tailings, thereby reducing overall recovery. The mineral grains within these particles may be fine grained or have a bimodal GSD of the valuable mineral(s) that may result from either inequigranular grains in one ore or blended material from ores with different size distributions where the target grind size is optimized for the largest of the distribution sizes. Alternatively, they may arise from the processing of a different ore type that requires finer grinding than the current ore's target grind size. These may not be recovered in the flotation circuit because they may

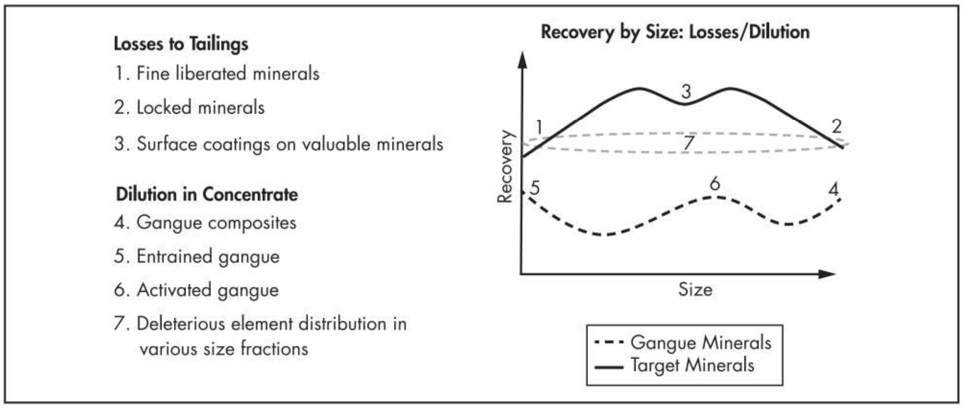

Adapted from Cropp et al. 2013, with permission from the Australasian Institute of Mining and Metallurgy

Figure 18 Summary of common causes for lower-than-anticipated grade or recovery in the flotation concentrate (graph highlights these regions relative to particle size)

be too heavy to float or lack the free surface area to be collected.

- Fine particles largely consist of liberated mineral grains. They have a lower probability of particle–bubble collision and therefore have a reduced chance of being recovered. Some mineral species are more susceptible to this phenomenon than others. For example, chalcopyrite floats reasonably well, even at very fine particle sizes. However, fine pentlandite flotation is challenging, especially when trying to maintain the same selectivity against sulfide gangue as in the more floatable size range. Very fine gangue material may also be recovered by entrainment to the final concentrate.
- In the midrange, particles are typically considered to be fully or well liberated and therefore amenable to separation in a flotation circuit, with the ore minerals being recovered without significant degradation of grade; however, this is not always the case. Surface coatings can reduce the susceptibility of an ore mineral's surface-to-bubble adherence, reducing recovery, whereas concentrate grade may be lowered when the surfaces of gangue minerals become activated (e.g., by copper ions), causing them to float.

From this discussion, it can be concluded that there is an optimum particle size and degree of liberation for flotation recovery. Too little liberation results in poor recoveries in coarse size fractions, whereas too much liberation results in fine liberated particles being lost due to poor flotation recoveries at the fine end of the particle sizes.

Gravity Separation

Like flotation, gravity separation has an optimum particle size for recoveries. Figure 19 shows the typical operating size ranges for a range of gravity separation units.

From Figure 19, it is apparent that some unit operations are more efficient at coarse sizes, such as jigs, heavy media drums, and heavy media cyclones. Others are more efficient at the fine end, as represented by the Falcon, Knelson, and Kelsey jigs. Hence, like flotation, poor liberation needs to be corrected to the particle size at which the gravity concentrators work most efficiently, which is a characteristic of the ore as well as the concentration method being used. Minerals that are amenable to gravity separation tend to have higher specific gravity (e.g., cassiterite, ferroplatinum, native gold, electrum). This effect needs to be considered in the layout of the grinding circuit, lest the classifier in the circuit (e.g., cyclone) inversely classifies the heavies into the circulating load, leading to overgrinding of these minerals and lower gravity recovery. For this reason, it is common to see an open-circuit rod mill performing the duty of primary grinding, followed by a unit gravity recovery process before the ground ore is further ground to product size, in which case gravity gold recoveries approach 90% (Laplante et al. 1990). The operation of a gravity recovery process inside the circulating load of a grinding circuit improves the kinetics of downstream cyanidation (Laplante and Staunton 2004).

Another important point about gravity recovery in the case of gold is that not all of the assayed gold may occur as native gold or electrum, both of which respond to gravity concentration. Detailed studies on the selection and breakage of discrete gold and electrum grains in the presence of silicate gangue showed that the discrete gold and electrum were prone to folding as a breakage mechanism and that this was combined with a smearing effect in which some of the gold entered the silicates as a texture, making it nonamenable to gravity recovery (Banisi et al. 1991). Thus, the achievement of good liberation of gold grains does not necessarily guarantee good recovery thereof. In cases where the total gold assay of an ore is distributed between a gravity-recoverable fraction and a refractory (non–gravity recoverable) fraction, test work has to be performed on a sample of that ore to determine how much gold occurs in either category. This subject was studied in detail by Laplante et al. (1994, 1996) and resulted in a standard procedure called gravity-recoverable gold.

Leaching

Similar to flotation and other separation processes, tank leaching requires valuable mineral particles to have optimal liberation and particle size. Ultimately, the decision on whether there is sufficient liberation is an economic one driven by the amount of extraction that can be achieved at a given particle size (Petersen 2016). This in turn depends on the cost of the comminution versus the value of the metal recovered. In tank leaching where residence times are in the window period of hours, high degrees of liberation and fine particle sizes with a high surface area are generally desired. When tank leaching is used for concentrates, it can be assumed that the valuable

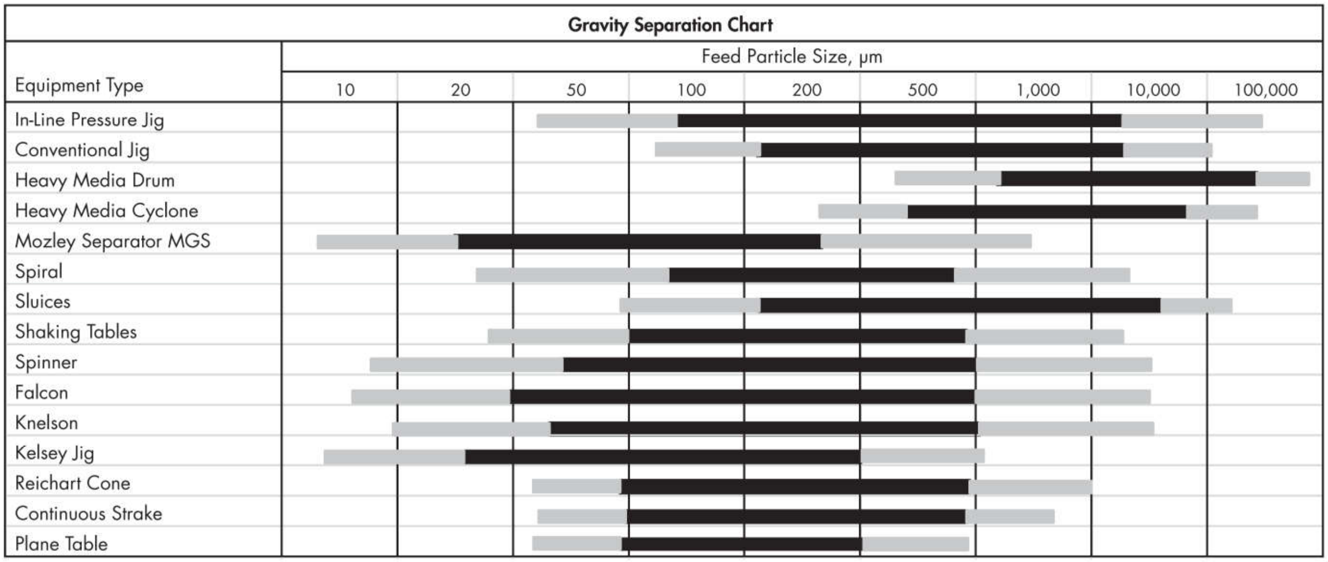

Adapted from Abols and Grady 2006

Figure 19 Operating sizes for a range of gravity separation processes

minerals are already well liberated because they have been recovered in a prior separation step such as flotation. This does not negate the need to measure the valuable mineral liberation itself, however, because the measurements provide accompanying information on the associated minerals (potentially flagging associations to deleterious minerals) or changes in valuable mineral deportment. Over and above is the certainty that the deportment and mineralogy of the valuable elements are amenable to leaching (e.g., refractory gold ores that need chemical pretreatment to liberate the gold from the crystal lattice of the host sulfide minerals) (Zhou et al. 2004; Vaughan 2004).

In the case of heap leaching, high degrees of liberation are not required for extraction, as the phase of interest need only be exposed to the leach liquor. Different processes have different cost–recovery curves, with the best example being the choice of flotation versus heap leaching for porphyry copper ores. In the case of flotation, ore feed is typically milled down to a P_{80} grind size of between 125 and 250 μm to achieve a copper recovery of between 85% and 95%. Heap leaching has a different cost–recovery curve, where ore is typically milled down to 25–75 mm and heap leach recoveries of 60%–80% are achieved. Flotation therefore requires a finer grind to achieve economic recoveries as compared to heap leaching because liberation in flotation is aimed at producing a significant proportion of liberated particles to achieve an economic grade–recovery curve. By contrast, heap leaching only requires enough liberation for the copper minerals to be exposed to the leach liquor. Hence, copper contained in complex particles is still leachable if there is sufficient surface exposure or cracks in the particles to allow the leach liquor to penetrate the internal minerals in the particle.

Unlike flotation and gravity separation, extraction from heap leaching does not suffer from the production of a large quantity of liberated particles in the fine size ranges during crushing. In heap leaching, however, there are good reasons for not having a large quantity of fines in a heap.

DIAGNOSIS OF LIBERATION PROBLEMS AND PROPOSED IMPROVEMENTS

There are many examples of the inclusion of additional milling capacity in a circuit. The particular location of the intervention in an existing circuit and the particle size obtained in most cases have been based on the mineralogy of the ore being processed, the liberation desired, and the point of maximum benefit identified. The following case studies provide examples and details of where liberation problems have been identified and the process improvements that resulted from the liberation studies. These examples are not comprehensive, and the reader should refer to the literature for others, particularly in the monograph "Process Mineralogy" (Becker et al. 2016).

Flotation

New Brunswick Mining and Smelting Corporation Ltd.

The New Brunswick Mining and Smelting Corporation operations near Bathurst, New Brunswick, Canada, were treating the largest zinc ore resource in the world from start-up in 1964 to shutdown in 2014. The ore consisted of 60% sulfide gangue (mostly as pyrite), 20% silicates, and 20% valuable minerals. Four salable concentrates were produced: lead, zinc, copper, and lead/zinc. Differential froth flotation was used to deliver these products from the grinding circuit product. Until 1998, the comminution circuit comprised two crushing stations, three rod mills, and three primary ball mills. Thereafter, these were all replaced by an autogenous grinding (AG) mill with secondary ball mills, the former being converted to semiautogenous grinding (SAG) in 1999 (Cormier and Cooper 2002).

A performance history of zinc grade and recovery at this site is shown in Figure 20 (Orford et al. 2005). Figure 20 shows three distinct domains of endeavor:

1. Back to basics—early 1980s to 1995
2. Point C—1995–2002
3. Six Sigma—after 2002

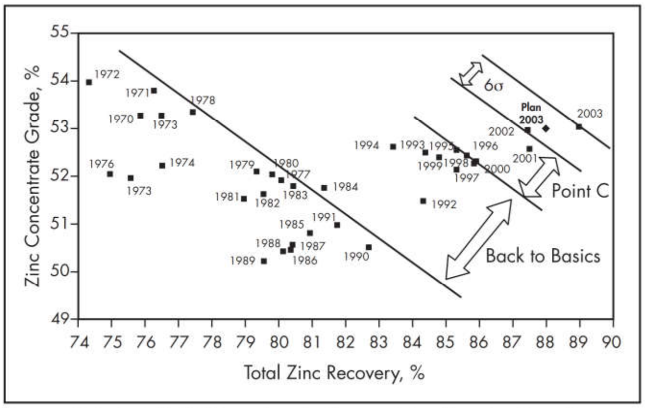

Source: Orford et al. 2005, reprinted with permission from the Canadian Institute of Mining, Metallurgy and Petroleum

Figure 20 Zinc grade and recovery performance history at the Brunswick operations

The improvements since 1990 were accrued from a range of focused efforts, including

- Staged flotation of the primary grinding product,
- Implementation of AG, and
- Streamlining of multiple process lines.

Supporting test work at various scales demonstrated that the baseline plant performance was less than optimum. From 1990 to 1995, improvements focused on optimizing equipment capability and reassessing reagents and control variables. The guideline here was to optimize the existing asset (equipment) before applying for capital to install new machinery. Effort was put into information on liberation, mineralogy, pulp and mineral surface chemistry, flotation kinetics, and entrainment.

From 1996 to 2000 (marked as point C in the figure), capital expenditure projects were approved and implemented at this site to improve the global competitiveness of the operation. The main features of these projects included the AG/SAG mill retrofit, paste backfill, stage grinding, and consolidation of the process into one continuous processing line.

At this stage, one of the tasks in the "staged grinding project" reported by Cormier and Cooper (2002) included the attainment of finer grinding from the existing grinding circuit by means of reducing the slurry density of the cyclone feed. The staged grinding part of the task was to insert the lead rougher float between the primary and secondary grinding stages to remove as much lead as possible from the downstream copper and zinc flotation stages.

Post-2002 saw the Six Sigma phase, which addressed smaller performance opportunities with better tools, such as the Six Sigma measurement system analysis, which, for example, was able to reduce the zinc grade in lead concentrate from 6.0% to 2.5% Zn.

An earlier investigation at the same site had already concluded that liberation was a limiting factor in metals recoveries. The behavior of minerals during flotation of this fine-grained, pyrite-rich, base metal ore was investigated in 1981 by studying the feeds, concentrate, and tailings from every flotation cell (Petruk and Schnarr 1981). The samples were analyzed for Zn, Pb, Cu, Fe, Ag, Sb, Sn, Bi, In, Hg, Mo, and As. Mass balances were computed, and recoveries of all metals from each cell, from each circuit, and from the mill were calculated. The percentages of sphalerite, galena, and chalcopyrite occurring as free grains in each product were determined with an image analyzer—as were size analyses for free mineral grains and middling particles—and were compared with screen analyses. The results showed that the behavior of minerals is defined much better by the recovery of free mineral grains than by the recovery of elements. The recovery of free sphalerite in the zinc circuit was 96%, whereas Zn recovery from the same circuit was 88%, the difference being due to unliberated sphalerite. The recovery of free sphalerite from the mill feed was 88% and Zn recovery was 78%. The recovery of free galena from the mill feed was 88% and Pb 64%. The recovery of free chalcopyrite was 75% and Cu recovery was 45%. Size analyses showed that more sphalerite and chalcopyrite could be liberated by regrinding, but the galena was so fine-grained that regrinding would not necessarily improve liberation. Silver occurs mainly in tetrahedrite and galena; the main loss in the tailings was due to large (+26 μm) and small (–1 μm) free and unliberated tetrahedrite grains.

Kennecott Utah Copper Concentrator

In cases when the ore types in a deposit are treated as blends, particular ore types can cause problems, and if the appropriate operating conditions cannot be identified, it can be better to process that ore type separately. Rio Tinto's Kennecott Utah Copper Concentrator (KUCC) is one of the world's longest-running and largest producing porphyry copper mines also rich in gold, silver, and molybdenum. Because of the quantity of ore being processed at any one time, the feed consists of several blends of its various ore types. In 2006, one of the ore types was identified as problematic, and a project was initiated to identify the causes (Triffett et al. 2008; Bradshaw et al. 2011, 2016).

The recovery from two ore types from KUCC was compared: a monzonite (MZME3) ore representing the ore with a typical copper and molybdenum recovery and a limestone skarn (LSN) ore with poor recoveries (see the reflected-light micrographs of samples in Figure 21). With similar amounts of total copper but very different recovery rates, the nature and proportions of the texture and gangue minerals were examined, including the particle size distribution after milling. Results showed that the LSN had a different particle size distribution, with more materials reporting to both the coarse and fine fractions, possibly due to the wider range of both harder (such as andradite and garnet) and softer minerals than those found in the MZME3 ore. The copper minerals were found to be finer in the LSN ore, allowing the potential for a greater quantity of unliberated copper-bearing grains in the coarse size fractions.

The theoretical grade–recovery curves produced from QEMSCAN mineralogical data shown in Figure 22 highlight the lower liberation of copper minerals in the coarse particles of the LSN ore compared to those of the MZME3 ore. These results are supported by the lower actual recovery to the flotation concentrate in laboratory tests seen in these fractions for the LSN ore shown in Figure 23.

The coarse size fraction in the LSN ore displays a lower grade–recovery curve than the equivalent fraction in the MZME3 ore due to the finer copper minerals staying locked (Bradshaw et al. 2011). Thus, it was also possible at KUCC

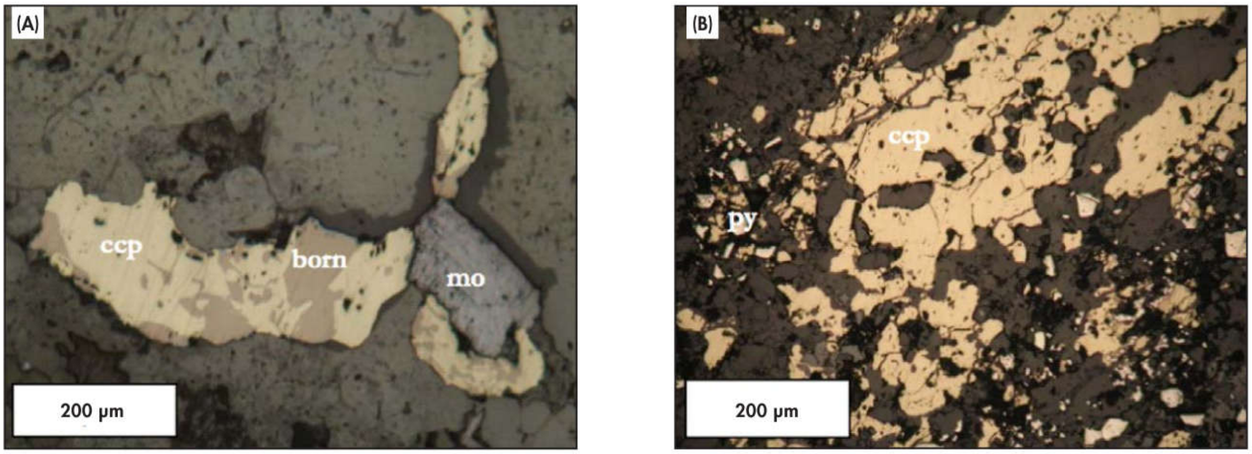

Source: Bradshaw et al. 2016

Figure 21 Reflected-light photomicrographs of (A) MZME3 ore and (B) LSN ore (Ccp = chalcopyrite; born = bornite; mo = molybdenite; py = pyrite)

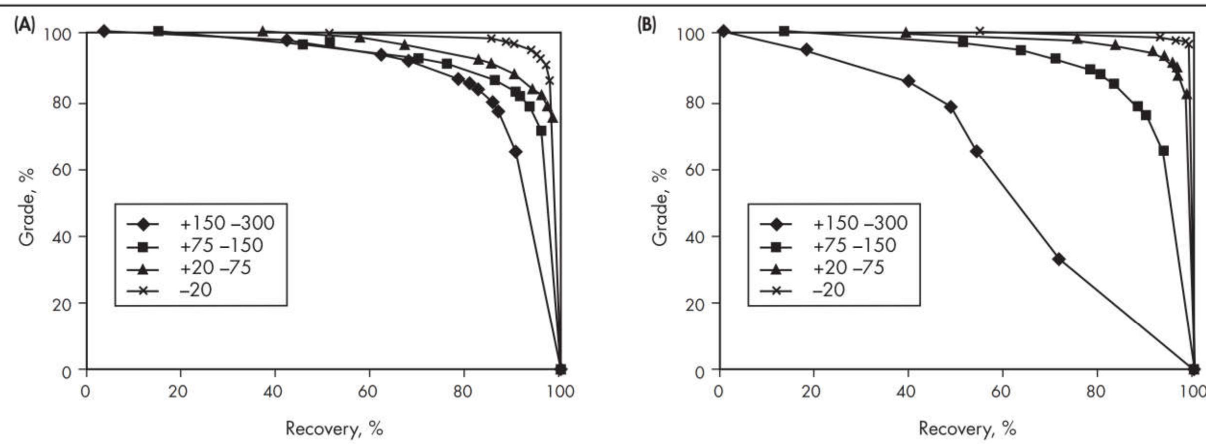

Source: Bradshaw et al. 2016

Figure 22 Theoretical grade–recovery curves based on the mineralogy of (A) the MZME3 ore and (B) the LSN ore

to identify the reasons for the poor performance of one of the LSN ores when it was processed in a blend; it was decided to process this ore type in batches and not to blend it.

Gravity Separation

The most oft-cited argument for installing a gravity circuit to recover gold in a plant is increased metallurgical recovery. The nature of the downstream circuit, as either flotation or cyanidation, greatly affects the impact of gravity recovery on overall metallurgical recovery. When installed inside the circulating load of a grinding circuit, the gravity recovery unit operation bleeds the high circulating load of gold that develops due to its high specific gravity—suffering inverse classification in the hydrocyclone (Laplante et al. 1994). Gold and electrum tend to fold rather than break in the grinding process due to their malleability. In a study on Hemlo ore, it was shown that the selection function of quartz was four times that of gold (Banisi et al. 1991). As a result, when gold particles respond to breakage in a grinding circuit, they tend to only move to the next screen size down in the particle size distribution, whereas quartz tends to break down to much finer size classes. This implies that free gold grains will have a longer residence time in the mill and that liberation measurements may not necessarily imply that this gold is immediately recoverable. Gravity-recoverable gold is limited above a certain lower sieve size below which the gravity recovery units tend to fail; thus, ultrafine liberated gold found by mineralogical measurements should not be added to the total of gravity-recoverable gold.

Leaching

In the case of heap leaching, the phases to be extracted do not require a high degree of liberation, as the aim is to obtain sufficient liberation for the leach liquor to contact the mineral phase of interest. This only requires surface liberation or internal cracks and pathways into the particle to allow liquor to flow into the particle. Hence, heap leach pads typically comminute to a particle size of 12.5–50 mm as compared to 150–200 μm for flotation. The case study described in this section shows a mineralogical and metallurgical comparison of three different ores leached in a column under identical leach conditions. This case study was reported by Latti and

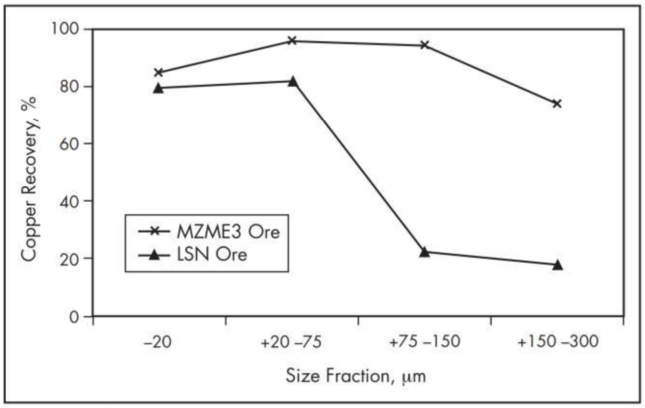

Source: Bradshaw et al. 2016

Figure 23 Copper recovery by size fraction for laboratory flotation tests of the MZME3 and LSN ores

Table 5 Leach conditions for three different ores

Ore	Feed Grade, % Cu	Ore Size, mm	Copper Extraction, % Cu	Acid Consumption, kg/t ore
Baseline	0.22	–12.5	67.7	108
Ore A	0.52	–12.5	29.4	60
Ore B	0.35	–12.5	51.0	232

Source: Latti and Wilkie 2016

Table 6 Mineralogy of the three ore feeds

	Percentage Mineral in Feed		
Mineral	**Baseline Ore**	**Ore A**	**Ore B**
Chalcopyrite	0.66	0.84	0.87
Bornite	0.00	0.20	0.06
Covellite	0.00	0.00	0.00
Chalcocite	0.00	0.16	0.01
Copper-arsenic sulfides	0.00	0.00	0.00
Other copper minerals	0.00	0.02	0.03
Pyrite	2.13	0.16	0.10
Other sulfides	0.13	0.08	0.01
Quartz	82.27	11.88	10.42
Plagioclase	0.03	15.46	33.08
Orthoclase	3.07	16.82	5.45
Altered orthoclase	0.41	27.43	8.92
Muscovite/illite	0.65	1.74	1.30
Biotite/phlogopite	4.21	3.21	12.23
Chlorite	0.86	4.22	14.32
Aluminum silicate	0.67	6.29	0.35
Amphibole	3.77	0.00	1.45
Andradite	0.00	0.00	0.02
Epidote	0.00	0.01	0.09
Calcite/dolomite	0.03	0.17	3.64
Iron oxide	0.43	0.47	2.90
Gypsum	0.00	8.00	0.00
Other	0.66	2.82	4.74

Source: Latti and Wilkie 2016

Wilkie (2016). Table 5 summarizes the leach conditions and extractions obtained from the three different ores. Although all three ores were crushed to the same particle size of 100% passing 12.5 mm, there was a large difference in the extractions obtained from the columns. Surprisingly, ore A had the highest feed grade of 0.52% Cu and the lowest extraction of 29.4%, whereas the baseline ore had the lowest feed grade at 0.22% Cu and the highest extraction of 67.7%. Ore B had a feed grade of 0.35% Cu and an extraction of 51%.

Table 6 compares the mineralogy of the three ore feeds. All three ores are chalcopyrite dominant, but ore A does contain a small amount of bornite and chalcocite. As it is chalcopyrite dominant, it can be concluded that the difference in extractions is not due to the different leaching rates between copper minerals but is rather due to a difference in the texture of the chalcopyrite. There is, however, a large difference in the gangue mineralogy between the two ores. The baseline ore is dominated by quartz with minor orthoclase, biotite/phlogopite and amphiboles, whereas ores A and B have considerably less quartz and significantly more plagioclase, orthoclase, biotite/phlogopite, and aluminum silicates. Ore B has more calcite/dolomite than either the baseline ore or ore A, which is important for acid consumption.

Figure 24 compares the size-by-size copper deportment of the three ore feeds. The baseline ore stands out as being different from both ore A and ore B in that the copper is uniformly distributed across all size fractions, whereas ores A and B have their copper heavily biased in the coarser size fractions. More than 40% of the copper in the baseline ore is in particles that are less than 4 mm. By contrast, only 25% of the copper in ore A is in particles finer than 4 mm, and ore B exhibits 34% in the fractions of less than 4 mm. Hence, although ore A has the highest grade, it also has the lowest proportion of copper in the fine fractions, which corresponds to the lowest extraction.

Conversely, the baseline ore has the lowest grade but the highest proportion of copper in the fine fractions of less than 4 mm, which corresponds to the highest extraction. The copper deportment in ore B is intermediate between the baseline ore and ore A with a corresponding intermediate extraction between the benchmark ore and ore A. It is clear from this result that ores A and B are liberation limited because the higher proportion of copper in the coarser 4-mm particles is unavailable for the leach liquor to contact the chalcopyrite grains. This can only be improved by crushing the ore more finely to send the larger proportion of copper in the coarse 4-mm fractions down to the fractions of less than 4 mm to make it available for leaching.

CONCLUDING REMARKS

This chapter shows that optimum liberation is a fundamental prerequisite to the separation and beneficiation of ores to achieve maximum recoveries across a range of mineral processing technologies. The first section of this chapter answered the question *Why is liberation critical to mineral processing?* The answer is that mineral ores, by their nature, are heterogeneous mixtures of ore minerals and gangue minerals, so to concentrate or extract the valuable mineral or metal, the ore must be broken down to a particle size where the mineral processing technology can efficiently concentrate or extract the valuable mineral or metal from the unwanted gangue minerals.

Because the optimum liberation size of a phase is a function of both the ore and the process technology being used, it

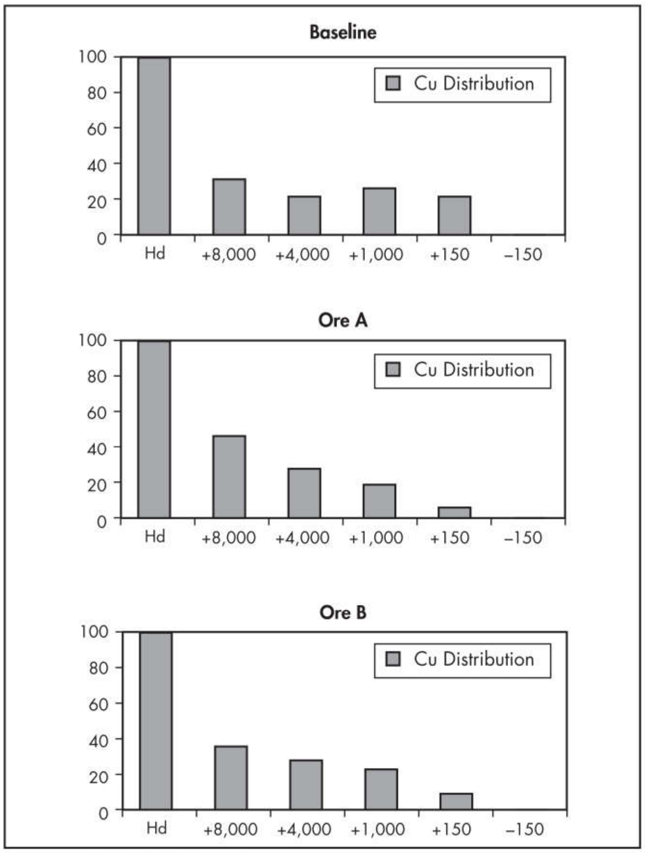

Source: Latti and Wilkie 2016

Figure 24 Size-by-size copper deportment for the three ore feeds

is important to measure the degree of liberation that the ore can produce at the optimum particle size for recovery. The second section of this chapter answered the question *How is liberation measured?* and discussed the two main methods of measurement: 2-D measurements performed on polished sections using manual and automated technologies, and 3-D measurements using either physical methods to produce liberation classes from heavy liquid separation or 3-D visualization of particles using tomography instruments. Each method was explored with respect to its strengths and weaknesses as well as the use of liberation modeling to determine the liberation properties of an ore at a given particle size.

The third section of this chapter answered the question *What is the best way to report liberation?* It provided a description of the traditional analysis using optical microscopy to classify particles in terms of proportions of liberated particles, binary particles with other minerals, and ternaries that are locked with two or more minerals. In addition to this classical approach to reporting liberation, commercially available automated SEM techniques provide additional ways of reporting liberation in the form of theoretical grade–recovery curves, liberation and association, false-color particle images, liberation spectrum, and CLYs. Examples of these forms were also presented.

The fourth section answered the question *When is there enough liberation?* Most mineral processing technologies have an optimum particle size for the efficient recovery of liberated and near-liberated particles, so it is important that the feed stream be prepared to maximize liberation within these particle size constraints. Not enough liberation will result in loss of recovery and grade due to poor exposure of the mineral of interest to the reagents being used to recover the mineral. Too much liberation may result in the liberated particles being too small for the mineral processing technology to efficiently recover fine particles. This section discussed the need for optimum liberation using a range of mineral processing technologies, including flotation, leaching, and gravity separation.

Finally, the fifth section of this chapter provided three case studies of diagnoses of liberation problems and the process improvements required to deliver a more optimum liberation solution.

REFERENCES

Abols, J.A., and Grady, P.M. 2006. Maximizing gravity recovery through the application of multiple gravity devices. Presented at the Gravity Concentration ’06 Conference, Perth, Australia, March 13–14.

Banisi, S., Laplante, A.R., and Marois, J. 1991. The behaviour of gold in the Hemlo Mines Ltd. grinding circuit. Presented at the 23rd Annual Meeting of the Canadian Mineral Processors, Ottawa, ON, Canada, January 22–24.

Barbery, G. 1984. Mineral liberation analysis using stereological methods: A review of concepts and problems. In *Applied Mineralogy*. Edited by W.C. Park, D.M. Hausen, and R.D. Hagni. New York: AIME. pp. 171–190.

Barbery, G. 1987. Random sets and integral geometry in comminution and liberation of minerals. *Miner. Metall. Process.* 4:96–102.

Barbery, G. 1991. *Mineral Liberation: Measurement, Prediction and Use in Mineral Processing*. Quebec City, QC: Les Editions GB.

Becker, M., Wightman, E.M., and Evans, C.L. (eds.). 2016. Process mineralogy. In *JKMRC Monograph Series in Mining and Mineral Processing No 6*. Brisbane, Queensland: Julius Kruttschnitt Mineral Research Centre.

Bradshaw, D.J. 2014. The role of “process mineralogy” in improving the process performance of complex sulphide ores. Presented at the XXVII International Mineral Processing Congress (IMPC 2014), Santiago, Chile, October 20–24.

Bradshaw, D., Triffett, B., and Kashuba, D. 2011. The role of process mineralogy in identifying the cause of the low recovery of chalcopyrite at KUCC. In *Proceedings of the 10th International Congress for Applied Mineralogy (ICAM)*, Trondheim, Norway, August 1–5. Berlin, Germany: Springer. pp. 71–80.

Bradshaw, D., Triffett, B., Latti, D., Wilkie, G., and Adair, B. 2016. Dealing with a problematic ore type at Kennecott Utah Copper Concentrator. In *JKMRC Monograph Series in Mining and Mineral Processing No. 6*. Edited by M. Becker, E. Wightman, and C. Evans. Brisbane, Queensland: Julius Kruttschnitt Mineral Research Centre. pp. 261–272.

Chayes, F. 1944. Petrographic analysis by fragment counting; Part 1, The counting error. *Econ. Geol.* 39(7):484–450.

Chayes, F. 1945. Petrographic analysis by fragment counting; Part 2, Precision of micro-sampling and the combination error of sampling and counting. *Econ. Geol.* 40(8):517–525.

Cormier, J.A., and Cooper, M. 2002. Implementation of stage grinding at the Brunswick concentrator. Presented at the 34th Annual Meeting of the Canadian Mineral Processors, Ottawa, ON, Canada, January 22–24.

Cropp, A., Goodall, W., and Bradshaw, D. 2013. The influence of textural variation and gangue mineralogy on recovery of copper by flotation from porphyry ore—A review. Presented at the Second AusIMM International Geometallurgy Conference (GeoMet 2013), Brisbane, Queensland, Australia, September 30–October 2.

Davy, P. 1984. Probability models for liberation. *J. Appl. Probab.* 21(2):260–269.

Efron, B. 1987. Better bootstrap confidence intervals. *J. Am. Stat. Assoc.* 82:171–185.

Evans, C.L. 2002. *Mineral Liberation Research at the JKMRC—Past, Present and Future.* P9 project report. Brisbane, Queensland: Julius Kruttschnitt Mineral Research Centre.

Evans, C.L., and Morrison, R.D. 2016. Mineral liberation. In *JKMRC Monograph Series in Mining and Mineral Processing No. 6*. Edited by M. Becker, E. Wightman, and C. Evans. Brisbane, Queensland: Julius Kruttschnitt Mineral Research Centre. pp. 133–147.

Evans, C.L., and Napier-Munn, T.J. 2013. Estimating error in measurements of mineral grain size distribution. *Miner. Eng.* 52:198–203.

Evans, C.L., Wightman, E.M., and Yuan, X.M. 2012. Characterising ore micro-texture using X-ray microtomography. Presented at the 44th Annual Meeting of the Canadian Mineral Processors, January 17–19.

Evans, C.L., Andrusiewicz, M.A., Wightman, E.M., Brennan, M., Morrison, R.D., and Manlapig, E.V. 2013. Simulating concentrators from feed to final products using a multi-component methodology. SME Preprint No. 13-094. Englewood, CO: SME.

Gaudin, A.M. 1939. *Principles of Mineral Dressing*. New York: McGraw-Hill.

Gay, S.L. 1996. Liberation modelling using particle sections. Ph.D. dissertation, University of Queensland, Brisbane, Queensland, Australia.

Gay, S.L. 2004. Simple texture-based liberation modelling of ores. *Miner. Eng.* 17(11–12):1209–1216.

Ghorbani, Y., Becker, M., Petersen, J., Mainza, A.N., and Franzidis, J.-P. 2013. Investigation of the effect of mineralogy as rate-limiting factors in large particle leaching. *Miner. Eng.* 52:38–51.

Gu, Y., Schouwstra, R.P., and Rule, C. 2014. The value of automated mineralogy. *Miner. Eng.* 58:100–103.

Gy, P.M. 1979. *Sampling of Particulate Materials—Theory and Practice*. Amsterdam: Elsevier.

Henley, K.J. 1983. Ore dressing mineralogy—A review of techniques, applications and recent developments. Presented at the First International Congress on Applied Mineralogy (ICAM '81), Johannesburg, South Africa.

Jackson, B.R., Gottlieb, P., and Sutherland, D.N. 1988. A method for measuring and comparing the mineral sizes of ores from different origins. Presented at the Third Mill Operators' Conference, Cobar, New South Wales, Australia.

Johnson, N.W. 2010. Existing methods for process analysis. In *Flotation Plant Optimisation: A Metallurgical Guide to Identifying and Solving Problems in Flotation Plants*. Edited by C.J. Greet. Melbourne, Victoria: Australasian Institute of Mining and Metallurgy. pp. 35–64.

Jowett, A. 1980. Formation and disruption of particle–bubble aggregates in flotation. In *Fine Particles Processing, Vol. 1*. Edited by P. Somasundaran. New York: AIME. pp. 720–754.

King, R.P. 1982. The prediction of mineral liberation from mineral texture. Presented at the XIV International Mineral Processing Congress, Toronto, ON, Canada.

King, R.P. 1983. Stereological methods for the prediction and measurement of mineral liberation. Presented at the First International Congress on Applied Mineralogy (ICAM '81), Johannesburg, South Africa.

King, R.P. 1990. Calculation of the liberation spectrum in products produced in continuous milling circuits. Presented at the 7th European Symposium on Comminution, Ljubljana, Slovenia.

King R.P. 2000. *Technical Notes 10: Mineral Liberation*. R.P. King. http://mineraltech.com/MODSIM/ModsimTraining/Module7/TechnicalNotes-10-Liberation.pdf.

Lamberg, P., and Vianna, S. 2007. A technique for tracking multiphase mineral particles in flotation circuits. In *Proceedings of the 7th Meeting of the Southern Hemisphere on the Mineral Technology, Ouro Preto, Brazil.* pp. 195–241.

Laplante, A.R., and Staunton, W.P. 2004. Gravity recovery of gold—An overview of recent developments. Presented at the International Symposium on the Treatment of Gold, Calgary, AB, Canada.

Laplante, A.R., Liu, L., and Cauchon, A. 1990. Gold gravity recovery at the mill of Les Mines Camchib Inc., Chibougamou, Québec. Presented at the 22nd annual meeting of the Canadian Mineral Processors, Ottawa, ON, Canada, January 16–18.

Laplante, A.R., Huang, L., and Vincent, F. 1994. Practical considerations in the operation of gold gravity circuits. Presented at the 26th annual meeting of the Canadian Mineral Processors, Ottawa, ON, Canada, January 18–20.

Laplante, A.R., Vincent, F., and Luinstra, W.F. 1996. A laboratory procedure to determine the amount of gravity recoverable gold—A case study at Hemlo Gold Mines. Presented at the 28th Annual Operator's Conference of the Canadian Mineral Processors, Ottawa, ON, Canada, January 23–25.

Latti, A.D. 2006. The textural effects of multiphase mineral systems in liberation measurement. Ph.D. dissertation, University of Queensland, Brisbane, Queensland, Australia.

Latti, A.D., and Wilkie, G. 2016. Mineralogy and leaching of copper ores. In *JKMRC Monograph Series in Mining and Mineral Processing No. 6*. Edited by M. Becker, E. Wightman, and C. Evans. Brisbane, Queensland: Julius Kruttschnitt Mineral Research Centre. pp. 291–302.

Leigh, G.M., Sutherland, D.N., and Gottlieb, P. 1993. Confidence limits for liberation measurements. *Miner. Eng.* 6(2):155–161.

Leigh, G.M., Lyman, G.J., and Gottlieb, P. 1996. Stereological estimates of liberation from mineral section measurements: A rederivation of Barbery's formulae with extensions. *Powder Technol.* 87:141–152.

Lotter, N.O., Whittaker, P.J., Kormos, L.J., Stickling, J.S., and Wilkie, G.J. 2002. The development of process mineralogy at Falconbridge Limited and application to the Raglan Mill. *CIM Bull.* 95:85–92.

Lotter, N.O., Baum, W., Reeves, S., Arrué, C., and Bradshaw, D.J. 2018a. The business value of best practice process mineralogy. *Miner. Eng.* 116:226–238.

Lotter, N.O., Evans, C.L., and Engström, K. 2018b. Sampling—A key tool in modern process mineralogy. *Miner. Eng.* 116:196–202.

Mariano, R.A., and Evans, C.L. 2015. Error analysis in ore particle composition distribution measurements. *Miner. Eng.* 82:36–44.

McIvor, R.E., and Finch, J.A. 1991. A guide to the interfacing of plant grinding and flotation operations. *Miner. Eng.* 4(1):9–23.

Miller, J.D., and Lin, C.L. 1988. The treatment of polished section data for detailed liberation analysis. *Int. J. Miner. Process.* 22:41–58.

Miller, J.D., Lin, C.L., and Cortes, A.B. 1990. A review of X-ray computed tomography and its application in mineral processing. *Miner. Process. Extr. Metall. Rev.* 7:1–18.

Miller, J.D., Lin, C.L., Hupka, L., and Al-Wakeel, M.I. 2009. Liberation-limited grade/recovery curves from X-ray micro CT analysis of feed material for the evaluation of separation efficiency. *Int. J. Miner. Process.* 93:48–51.

Morrison, R.D., and Gu, Y. 2016. X-ray computed microtomography. In *JKMRC Monograph Series in Mining and Mineral Processing No. 6*. Edited by M. Becker, E. Wightman, and C. Evans. Brisbane, Queensland: Julius Kruttschnitt Mineral Research Centre.

Napier Munn, T.J., Morrell, S., Morrison R.D., and Kojovic, T. 2005. *Mineral Comminution Circuits: Their Operation and Optimisation*. Indooroopilly, Queensland: Julius Kruttschnitt Mineral Research Centre.

Orford, I., Cooper, M., Larsen, C., Deredin, C., Gauthier, J.-G., Fortin, C., Côté, L., Trusiak, A., and Scott, D. 2005. The approach to process improvements at Brunswick Mine. Presented at the 37th annual meeting of the Canadian Mineral Processors, Ottawa, ON, Canada, January 18–20.

Petersen, J. 2016. Heap leaching as a key technology for recovery of values from low-grade ores—A brief overview. *Hydrometallurgy* 165:206–212.

Petruk, W. 2000. *Applied Mineralogy in the Mining Industry*. Amsterdam: Elsevier.

Petruk, W., and Schnarr, J.R. 1981. An evaluation of the recovery of free and unliberated mineral grains, metals and trace elements in the concentrator of Brunswick Mining and Smelting Corp. Ltd. *CIM Bull.* 74(833)132–159.

Spencer, S., and Sutherland, D. 2000. Stereological correction of mineral grade distributions estimated by single section of particles. *Image Anal. Stereol.* 19:175–182.

Stewart, P.S.B., and Jones, M.P. 1977. Determining the amounts and the compositions of composite (middling) particles. Presented at the Twelfth International Mineral Processing Congress, São Paulo, Brazil.

Subasinghe, G.K.N., and Dunne, R. 2016. Predictive model of mineral liberation for geometallurgical applications. Presented at the Third AusIMM International Geometallurgy Conference, Perth, Australia, June 15–16.

Sutherland, D.N. 1989. Batch flotation behaviour of composite particles. *Miner. Eng.* 2(3):351–367.

Sutherland, D., Gottlieb, P., Jackson, R., Wilkie, G., and Stewart, P. 1988. Measurement in section of particles of known composition. *Miner. Eng.* 1(4):317–326.

Sutherland, D.N., Gottlieb, P., Wilkie, G., and Johnson, C.R. 1991. Assessment of ore processing characteristics using automated mineralogy. Presented at the XVII Mineral Processing Congress, Dresden, Germany.

Trahar, W.J. 1981. A rational interpretation of the role of particle size in flotation. *Int. J. Miner. Process.* 8:289–327.

Triffett, B., Veloo, C., Adair, B.J.I., and Bradshaw, D.J. 2008. An investigation of the factors affecting the recovery of molybdenite in the Kennecott Utah copper bulk flotation circuit. *Miner. Eng.* 21:832–840.

Van der Plas, L., and Tobi, A.C. 1965. A chart for judging the reliability of point counting results. *Am. J. Sci.* 263:87–90.

Vaughan, J.P. 2004. The process mineralogy of gold: The classification of ore types. *J. Miner. Met. Mater. Soc.* 56:46–48.

Vos, C.F. 2017. The effect of mineral grain textures at particle surfaces on flotation response. Ph.D. thesis, University of Queensland, Brisbane, Queensland, Australia.

Wiegel, R.L., and Li, K. 1967. A random model for mineral liberation by size reduction. *Trans. SME* 238:179–189.

Wightman, E.M., and Evans, C.L. 2013. Representing and interpreting the liberation spectrum in a processing context. *Miner. Eng.* 61:121–125.

Wightman, E.M., Evans, C.L., Becker, M., and Gu, Y. 2016. Automated scanning electron microscopy with energy dispersive spectrometry. In *JKMRC Monograph Series in Mining and Mineral Processing No. 6*. Edited by M. Becker, E. Wightman, and C. Evans. Brisbane, Queensland: Julius Kruttschnitt Mineral Research Centre. pp. 97–107.

Wilkie, G.J. 2016. Assessing the sorting potential of mineral sulphide ores. Ph.D. dissertation, University of Queensland, Brisbane, Queensland, Australia.

Zhou, J., Jago, B., and Martin, C. 2004. *Establishing the Process Mineralogy of Gold Ores*. SGS Technical Bulletin 2004-03. Geneva, Switzerland: SGS Lakefield Research Limited.